JVSTB Journal of Vacuum Science & Technology B

Extreme ultraviolet lithography: A review

Banqiu Wu and Ajay Kumar

Citation: Journal of Vacuum Science & Technology B **25**, 1743 (2007); doi: 10.1116/1.2794048
View online: http://dx.doi.org/10.1116/1.2794048
View Table of Contents: http://scitation.aip.org/content/avs/journal/jvstb/25/6?ver=pdfcov
Published by the AVS: Science & Technology of Materials, Interfaces, and Processing

REVIEW ARTICLE

Extreme ultraviolet lithography: A review

Banqiu Wu[a] and Ajay Kumar
Applied Materials, Inc., Building 81, M/S 81505, 1285 Walsh Ave., Santa Clara, California 95050

(Received 4 September 2007; accepted 12 September 2007; published 11 October 2007)

Extreme ultraviolet lithography (EUVL) was thoroughly reviewed over a broad range of topics, including history, tools, source, metrology, condenser and projection optics, resists, and masks. Since 1988, many studies on EUVL have been conducted in North America, Europe, and Japan, through state sponsored programs and industrial consortiums. To date, no "show stopper" has been identified, but challenges are present in almost all aspects of EUVL technology. Commercial alpha lithography step-and-scan tools are installed with full-field capability; however, EUVL power at intermediate focus (IF) has not yet met volume manufacturing requirements. Compared with the target of 180 W IF power, current tools can supply only approximately 55–62 W. EUV IF power has been improved gradually from xenon- to tin-discharge-produced plasma or laser-produced plasma. EUVL resist has improved significantly in the last few years, with 25 nm 1:1 line/space resolution being produced with approximately 2.7 nm (3σ) line edge roughness. Actual adoption of EUVL will depend on the extension of current optical lithography, such as 193 nm immersion lithography, combined with double patterning techniques. Mask fabrication and application technologies may be the most substantial challenges. Creating a defect-free EUVL mask is currently an obstacle to its application, although a combination of removable pellicle and thermophoretic protection may overcome nonpellicle challenge. Cost of ownership is a critical consideration for EUVL; nevertheless, it has been predicted that EUVL may be in pilot production at 32 nm and in large-scale production at 22 nm with the capability to extend to the next technology node. © *2007 American Vacuum Society.* [DOI: 10.1116/1.2794048]

I. INTRODUCTION

Lithography technology was introduced to the semiconductor industry when the integrated circuit (IC) was invented in 1958. As technology advanced and feature size shrank, the wavelength of exposure light decreased several times. Original lithography used visible *g*-line (436 nm) and ultraviolet *i*-line (365 nm) lights produced by mercury arc lamps. When IC feature size shrank to approximately half a micron, these wavelengths met a significant challenge, which gave rise to deep ultraviolet 248 nm KrF and 193 nm ArF excimer lasers for lithography. Now, state-of-the-art lithography is a combination of 193 nm lithography and immersion technology. For smaller feature ICs, shorter wavelength lithography, known as next-generation lithography (NGL), was studied using 157 nm wavelength, extreme ultraviolet (EUV) light (e.g., 13.5 nm wavelength), x ray (0.4 nm), and even shorter wavelengths of electron and ion beams. Regardless of which method is ultimately adopted for NGL, throughput, cost of ownership, and imaging quality requirements must be satisfied.

While the wavelength range of EUV and soft x ray is not clearly defined, the former falls between 50 and 5 nm wavelengths and the latter between 5 and 0.2 nm wavelengths.[1]

Soft x-ray projection lithography, presently known as extreme ultraviolet lithography (EUVL), was proposed in 1988,[2] and experimentally investigated thereafter.[3,4] In these original studies, a synchrotron radiation source and polymethyl methacrylate (PMMA) resist were used to obtain 200 nm resolution.[3] In 1991, a compact laser plasma source was successful in proving EUVL feasibility.[5,6] In 1993, the Optical Society of America held a Topic Meeting of Extreme Ultraviolet (EUV) Lithography, where soft x ray and EUVL were referred to interchangeably, causing much confusion. Since 1994, EUVL has been used worldwide, replacing previously used soft x-ray projection lithography.

Compared with other NGL methods, such as proximity x-ray lithography, electron projection lithography, and ion projection lithography, EUVL is a new member of NGLs. Because it possesses special optical advantages, known as the natural extension of optical lithography, EUVL development has been relatively fast. Most other NGLs require 1X membrane masks, but EUVL uses masks with four- or five-fold image reduction, which makes mask fabrication feasible with current technology. Reflective optics have been used in EUVL optical systems, because all available materials are strong absorbers of EUV light and no materials are transparent enough to make use of refractive optics. EUV light is

[a]Electronic mail: banqiu_wu@amat.com

reflected on multilayer mirrors, i.e., the Bragg reflectors, usually consisting of molybdenum and silicon (Mo/Si) multilayer.

In the early and mid-1990s, systematic research was mainly performed by the Lawrence Livermore National Laboratory (LLNL),[7–21] Sandia National Laboratory (SNL),[11,22–26] and Lawrence Berkeley National Laboratory (LBNL).[27–30] as well as AT&T Bell Laboratories[31–36] and several universities.[37–41] In 1997, an industrial consortium, EUV LLC, was formed by Intel, Motorola, and Advanced Micro Device, to continue work on EUVL. At the same time, Virtual National Laboratories was also formed by LLNL, SNL, and LBNL to conduct a program sponsored by EUV LLC.

In Europe, an industrial consortium, Extreme Ultraviolet Concept Lithography Development System (EUCLIDES), was formed in 1998 by ASM Lithography (ASML), Carl Zeiss, and Oxford Instruments. Since then, EUVL studies in Europe have made significant progress, with ASML leading.

In Japan, original studies on EUVL were performed in NTT LSI Laboratories, and publications were found dating from 1989. Other EUVL pioneer work was carried out by Nikon and Hitachi around 1990. The Association of Super-Advanced Electronics Technologies (ASET) was established in 1996, launching its EUVL program in 1998. The Extreme Ultraviolet Lithography System Development Association was established in 2002. Many early EUVL studies in Japan were conducted in the 1990s.[3,42–44]

The extension of optical lithography has delayed adoption of EUVL and other NGL technologies. When it was proposed, EUVL was planned for the 100 nm technology node. In 1997, implementation was predicted for the 65 nm node. Further extension of optical lithography pushed predicted implementation out to the 45 nm node and beyond. Immersion exposure technology makes it feasible for 193 nm wavelength lithography to be used for the 45 nm technology node. This has delayed EUVL application again and has caused the industry to abandon 157 nm lithography. Now it is predicted that EUVL will have some pilot-scale applications at the 32 nm technology node or be used in full production for the 22 nm half-pitch technology node. Figure 1 shows the number of publications on various aspects of EUVL issued during the past 20 years. The main topics are EUV source, optics, mask, multilayer coating, resist, metrology, reticle handling, and contamination control (included in related subjects).

Although EUVL implementation has been repeatedly delayed, optical lithography has its inherent limit in resolution and depth of focus, shown by the following two equations:

$$R = k_1 \frac{\lambda}{\mathrm{NA}}, \tag{1}$$

$$\mathrm{DOF} \approx k_2 \frac{\lambda}{(\mathrm{NA})^2}, \tag{2}$$

where R is resolution, λ is wavelength, NA is numerical aperture, k_1 and k_2 are constants, and DOF is depth of focus.

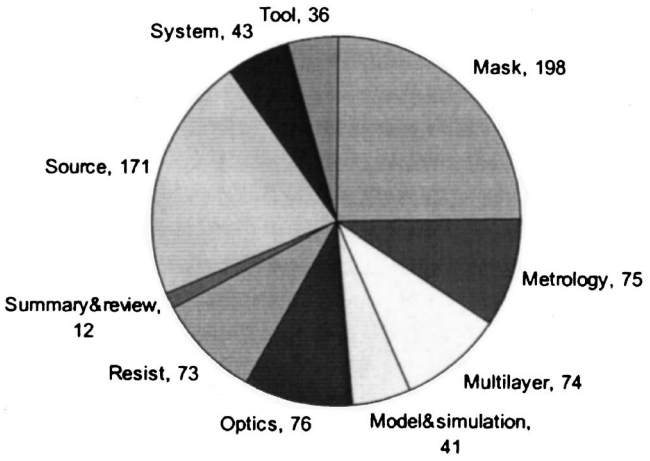

FIG. 1. Classification of EUVL-related publications.

By using immersion exposure technology and high NA, resolution can be improved significantly. Presently NA is as high as 1.35, and may increase to ~1.7 for 32 nm node technology. On the other hand, high NA values will decrease the depth of focus significantly, making operation more difficult.

EUVL technology includes EUV resist technology, EUV aligners or printers, and EUV masks, as well as metrology, inspection, and defectivity controls. In abandoning 157 nm lithography, the industry has created a technological jump from 193 to 13.5 nm wavelength, creating complex challenges across the board.

While the range of EUV wavelengths is broad, the most common ones are 11.3–11.6 nm, corresponding to a Mo/Be multilayer reflective mirror, and 13.3–13.6 nm, corresponding to a Mo/Si multilayer reflective mirror. To date, the Mo/Si multilayer for 13.5 nm EUV is the main candidate. Theoretically, the thickness of a pair of layers is half the wavelength. Therefore, for 13.5 nm EUV light, the Mo/Si thickness is approximately 6.75 nm (e.g., Mo 2.7 nm and Si 4.1 nm); for 11.4 nm EUV, Mo/Be thickness is 5.7 nm (Mo 2.3 nm and Be 3.4 nm).

EUVL was introduced as a high k_1 [in Eq. (1)] technology, thus it offers potential extendibility to smaller feature size nodes (see Table I).[45] For a conservative k_1 of 0.40 and 0.25 NA, resolution based on Eq. (1) can reach 22 nm half-pitch features. When using an aggressive optical design with 0.45 NA and a k_1 of 0.32, 10 nm half-pitch features can be printed.[46] This possibility gives EUVL a significant resolution advantage, compared with 193 nm optical lithography.

TABLE I. Target technology node and potential extendability of NA and k_1 values (Ref. 45).

Node\NA (nm)	0.25	0.35	0.5
32	0.59	0.83	1.19
22	0.41	0.57	0.81
16	0.30	0.41	0.59
11	0.20	0.29	0.41

TABLE II. Top three challenges in EUVL implementation.

Top Challenges	2002	2003	2004	2005	2006
First	Source output	Source output	Availability of defect-free mask	Resist resolution, sensitivity, and LER met simultaneously	Reliable high power source and collector module
Second	Defect-free ML mask blank manufacturing, including inspections	Defect-free ML mask blank manufacturing, including inspections	Lifetime of source component and collector optics	Collector lifetime	Resist resolution, sensitivity, and LER met simultaneously
Third	Source and condenser optics reliability	Optics reliability	Resist resolution, sensitivity, and LER met simultaneously	Availability of defect-free mask	Availability of defect-free mask
Fourth	Cost of ownership of EUVL	Projection and illuminator optics lifetime	Reticle protection during storage, handling and use	Source power	Reticle protection during storage, handling and use
Fifth	Defect-free pattered mask manufacturing/ commercial availability	Resist resolution, sensitivity and LER	Source power	Reticle protection during storage, handling and use	Projection and illuminator optics quality and lifetime

However, we should not be so optimistic about EUVL applications. Although it is now agreed that there is no show-stopper for EUVL technology, many critical challenges exist. The EUVL Symposium lists the top challenges every year, as shown in Table II. These challenges will have to be overcome before EUVL implementation becomes practical.

II. EUV EXPOSURE TOOLS

EUVL as a concept and design was proposed in 1988 by Hawryluke and Seppala at Lawrence Livermore National Laboratories[2] and the feasibility of the method and multilayer optics were examined experimentally at NTT LSI Laboratories in the following year.[3] EUV lights with wavelengths of 4.5–7.0 and 11.5–13.0 nm created from a synchrotron radiation source were used for exposure on PMMA and bilayer resists. Reflecting mask and Schwarzschild optics were used with 500 nm features obtained. In 1990, 100 nm resolution was obtained at AT&T Bell Laboratories by using PMMA resist and a transmission mask (membrane mask) as well as synchrotron radiation at 14 nm wavelength.[4]

EUV exposure tool design involves many new challenges. Stage in high vacuum condition is one of them. EUV optics fabrication was also very challenging. In the 1990s, EUV optics, related metrology, and light source presented the greatest challenges and development of a commercial EUVL aligner was a very high risk project. Against this background, EUV LLC developed the first EUV full-field exposure tool, Engineering Test Stand (ETS), to demonstrate the feasibility and capability by 2001.[47–51] Figure 2 shows a cross-sectional view of the ETS, its critical components, and EUV beam path.[52] It is a vacuum-compatible step-and-scan system with a four-mirror, four times reduction, ring-field design, numeral aperture of 0.1, and critical dimensions of objectives in the 70–100 nm range. It uses laser-produced plasma (LPP) as its EUV source. In static imaging mode, 100 nm isolated and dense features were obtained on this tool. The ETS field size is 24×32.5 mm^2. The first phase of tool integration has $\lambda/14$ wave front error (WFE) with the final projection system at $\lambda/24$ WFE.[49] The EUV source uses a xenon injection laser target. Figure 3 shows the ETS arc illuminator and full-field mask coverage in step-and-scan mode.[53]

Although it could not meet the specifications of EUV lithography production tool, it proves the feasibility of this

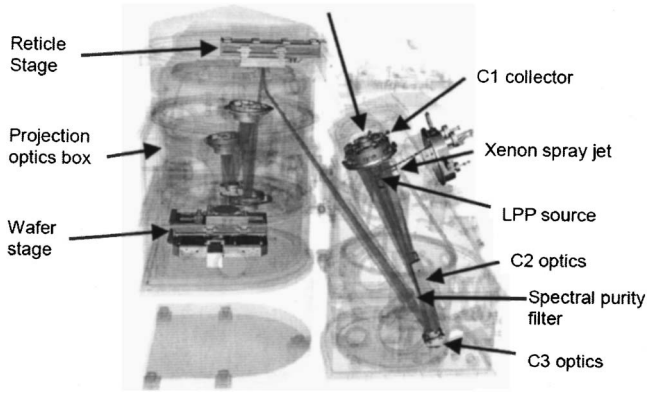

FIG. 2. Cross-sectional view of the ETS tool, its major components, and the EUV beam path.

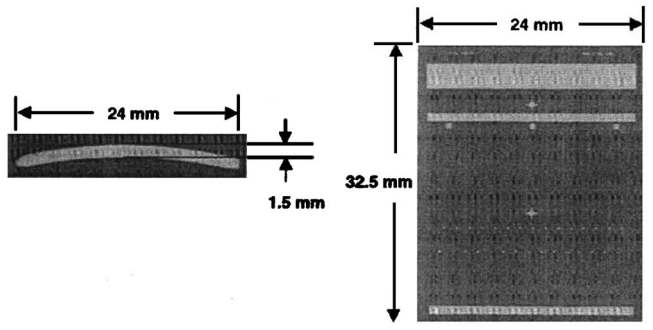

FIG. 3. ETS 28° arc illuminator (left) and mask coverage of the full-field in step-and-scan mode (the full field is extendable to 32.5 mm in the scanned dimension).

new technology and shows the promising future, which convinces the industry to move forward on this technology.

In Europe, EUCLIDES completed its first-phase EUVL project between 1998 and 2000.[54] During this phase, technical solutions were developed to overcome EUVL challenges, including mirror substrate, high reflectivity multilayer coatings, resist outgassing reduction schemes, and vacuum stages. In 2001, ASML (system integration), Carl Zeiss (optics), and their partners began to design and realize an alpha exposure tool.[55] In 2006, alpha-demo (AD) EUVL steppers were installed in IMEC and SEMATECH North in New York. This was a symbolic event showing that EUVL was advancing toward industrial production. The steppers were full-field size (26×33 mm^2), but EUV power at intermediate focus (IF) was only 15 W and needed improvement. The tool optics used six mirrors and $4\times$ demagnification. The maximum NA was designed to be 0.25 with 50 nm resolution.[55] It used tin-discharge-produced plasma (DPP) EUV light source.[56]

In Japan, ASET started an EUVL program in October 1998. Since then, Nikon has been working on mirror machining and multilayer coating. In 2001, Nikon investigated the feasibility of EUV scanners and planned to use six-mirror projection optics, with full-field size, and resist sensitivity of 2 mJ/cm^2.[57] They are presently developing a full-field exposure tool, EUV1; prototype projection optics were completed in spring 2007.[58,59] The tool uses a xenon DPP EUV light source and has a tight control of flare of 10%.[59]

Due to the very high costs of full-field EUV exposure tool, availability is limited. In order to help EUV resist and mask development, a small-field EUV exposure tool with high NA and resolution is needed. Therefore, concurrently with ETS, a microexposure tool was developed for 30 nm feature printing to provide a test bed for resist development.[48] The optics were developed through collaboration between Carl Zeiss and Lawrence Livermore National Laboratory.[55] It was operational from 2004 with a NA of 0.3 and demagnification of 5.[60] By 2005, it had obtained 25 nm line/space features with line edge roughness (LER) of 3 nm.[61]

Similarly, Exitech developed a microexposure stepper (MS-13) in 2004 with a NA of 0.3, demagnification of 5, and field size of 0.6×0.2 mm^2.[62] The tool was designed for resist testing and technology evaluation at the 32 nm node and beyond. It was installed in RP1 fab of Intel Corp., Hillsboro, Oregon, and the EUV Resist Test Center at the NanoFab North facility of SEMATECH North, Albany, New York.[63] At the same time, Exitech also developed a mask imaging actinic microscope for inspection and printability studies of amplitude and phase defects on blank and patterned EUVL masks. It has the capability to capture aerial images from EUV masks with illumination and image characteristics that emulate full-field production scanner tools.[63]

HINA, another small-field EUV exposure tool, with projection optics Set 3 was developed by Nikon in 2005.[64] The HINA-3 has a NA of 0.3, image field of 0.3×0.5 mm^2, WFE of 0.7 nm rms, and mid-spatial frequency roughness of 0.17 nm rms. This tool obtained 30 nm line and space patterns. Another small-field exposure tool was shipped to SELETE in 2007.[65] The tool has a field size of 0.6×0.2 mm^2 and two-mirror projection optics.

TABLE III. 2006 AD specifications.

Wavelength	13.5 nm
NA range	0.15–0.25
Field size	26×33 mm^2
Wafer size	300 mm
Reduction ratio	4:1
Flare	16%
Dense L/S	40 nm
Isolated lines	30 nm
Isolated contact	55 nm
Overlay	12 nm
Throughput	~10 wafers/h

Table III gives specifications of the state-of-the-art full-field exposure tool.[56] To date, it has not met production requirements. The greatest challenge in an EUV aligner is the EUV source power supply, which is currently less than half of the production requirement. Flare from EUV optical system is also very challenging, while stability and lifetime of the multilayer coating is yet another significant challenge. EUV preproduction exposure tool manufactured by ASML will be available in 2009. More details will be discussed in the following individual sections.

III. EUV SOURCE

Basic requirements and challenges related to the EUV light source are high enough in-band EUV power, prolonged stability, hot-spot size, collectable angle, acceptable contamination control, and minimum damage to the collector optics. Adequate in-band EUV power supplied by the source is the key for volume-production throughput and cost of ownership. After EUVL became the leading NGL in the late 1990s, the EUV source was studied extensively.[66–73] Because of the EUV absorption, the source chamber, optical chamber, and wafer printing chamber are in the same vacuum level without filter, necessitating strict debris or contamination control.

A synchrotron source was used for the original pioneer studies.[3,4] Its advantage is that it does not require periodic replacement of key components such as DPP and LPP sources, but its high cost and large space requirement limited its practical use in production tools. DPP and LPP sources are the main candidates for EUVL. These sources are based on high-temperature emitting plasmas, with several 100 000 K temperatures.[69] LPPs were widely studied[8–11,22,37,38] and applied on the ETS tool. Later, DPP was studied and used on the AD tool. A thorough calculation for the EUVL source was made.[74]

EUV source power is mainly determined by resist sensitivity. EUV resist with sensitivity of 5 mJ/cm^2 requires greater than 115 W, 2% bandwidth IF power to enable more than 100 wafers/h scanner throughput. Resist with sensitivity of 10 mJ/cm^2 requires greater than 180 W, 2% band-

width IF power.[75] However, collectable EUV power is very limited. For an EUV power of 645 W at 2π sr solid angle within 2% bandwidth, only 42 W IF power were obtained.[76]

There are two basic applications for EUV sources. One is as light source for EUVL exposure tools. For this application, very high EUV power is needed. Another use is for EUVL system characterization, including metrology tool applications. In this case, EUV power can be met relatively easily.

The EUV source is fundamental to EUVL success. In the mid- 1990s, KrF laser and high-Z targets (Re, Nb, W, and Ta) were used for high EUV spectra with laser power of 3×10^{12} W/cm^2.[2,77,78] With 0.85% conversion efficiency at 2% bandwidth, 550 mW EUV was obtained. Generally, a high element number corresponds with high EUV conversion efficiency. However, these high-Z elements tend to contaminate the chamber. Centrifugal techniques are common for removing contamination, but it is difficult to obtain satisfactory control. EUV light filters were also studied.[74] The 50% transmission of 13.5 and 11.5 nm EUV requires 400 nm thickness of Si and Be. Unfortunately, such a thin film and 50% transmission are not acceptable to the industry.

The contamination from high-Z solid targets led to studies of liquid targets.[79–81] Contamination control when using liquid xenon is better than for a solid target, but the conversion efficiency is significantly lower. Two parameters are responsible for the final EUV IF power: conversion efficiency and solid angle captured by condenser. Because xenon is also a high-Z element, it was expected that this liquid would yield high conversion efficiency. Besides xenon, liquid water[82] combined with LPP was also examined, but demonstrated similarly low conversion efficiency.[79]

Among all target materials, tin, xenon, and lithium are the most promising candidates. However, lithium is a line emitter.[66] Although it has 13.50 nm wavelength radiation, the linewidth is only 0.03 nm. In the EUVL optical system, this means that a very small thickness change on the multilayer can produce significant reflectivity changes. This property, therefore, eliminates lithium from consideration as an EUV source in lithography.

Xenon's emission spectra were theoretically studied.[68] The 13.5 nm wavelength with 2% bandwidth was mainly emitted by $4d \rightarrow 5p$ transition, but the emission of $4p^6 4d^8 \rightarrow (4p^5 4d^9 + 4p^6 4d^7 4f)$ line group near 11 nm is significantly stronger than the $4d \rightarrow 5p$ transitions occurring near 13.5 nm. This intrinsic property limits the conversion efficient (CE) of a xenon target. Thus far, the typical CE of a xenon target has been approximately 1%, and it seems impossible to approach the industrial requirement of 3%.

EUV radiation materials are critical for increasing conversion efficiency. Tin is widely accepted as a better radiator than xenon with a much better spectral distribution of lines in the EUV, as shown in Fig. 4.[70] Candidates among gaseous tin compounds are SnH_4 and $(CH_3)_4Sn$.[83,84]

DPP has been extensively studied and is a promising candidate.[70,85–91] Fundamentals and limits for the EUV emission of pinch plasma sources for EUVL lithography were studied. Figure 5 is a schematic of a DPP EUV source.[71] High conversion efficiency and high EUV power are the main advantages of DPP EUV source. The main concerns are plasma electrode lifetime and debris control. By 2004, EUV IF power produced by DPP had grown to 44 W using tin and 22 W using xenon. However, there is still a way to go to achieve high-volume manufacturing power levels for EUVL.[70] Conversion efficiency of a tin source is about twice that of a xenon source, but the optical protection against debris is more difficult.

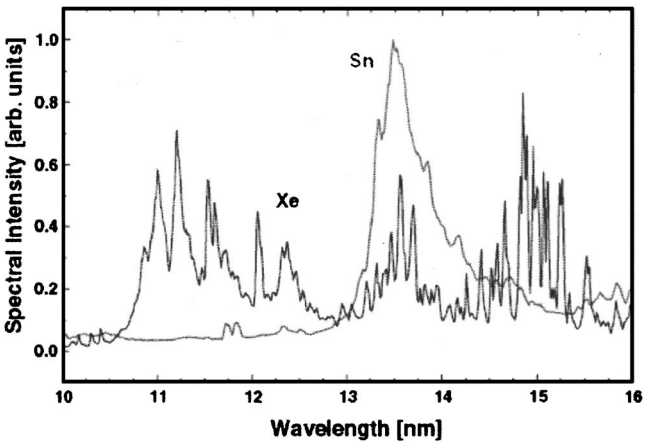

FIG. 4. Comparison of Xe and Sn EUV emission spectra from discharge-produced plasma generated under identical excitation conditions.

Consumption of the insulator and electrode in a DPP source system is a very challenging issue. It results from physical damage, chemical reaction, and bombardment, as well as melting and evaporation. The DPP small electrode area is subjected to thermal loads as high as 50 kW/cm^2.[92]

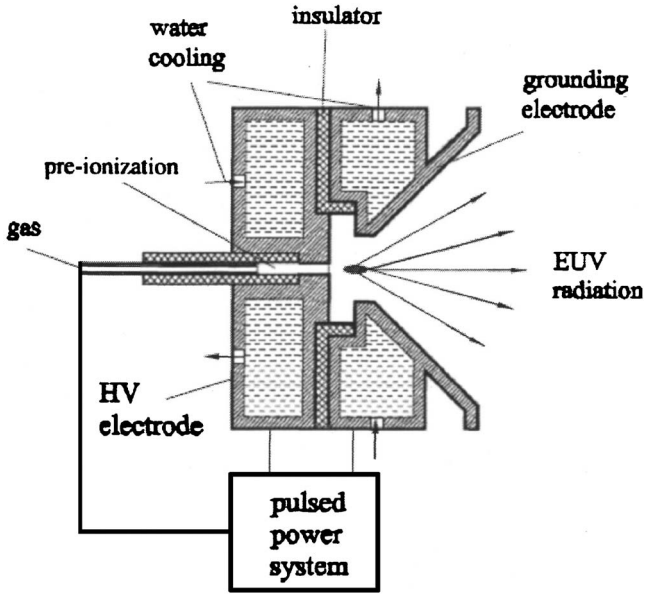

FIG. 5. Schematics of a discharge-produced plasma EUV source.

The repetition rate also plays an important role in obtaining high EUV power. By 2002, the repetition rate up to 3 kHz was obtained,[88] rising to 4 kHz by 2003.[89]

Simulations of an EUV source using DPP were also conducted.[93,94] Dense plasma focus, previously used primarily in fusion studies, was also studied for EUVL application.[72] Results showed significantly higher plasma temperatures due to its shorter pulse length and higher output voltage. Positive polarity, i.e., the central electrode as anode, was compared with negative polarity. The former benefits electrode heating, erosion, and contamination control, and the latter aids efficient discharge initiation.

Surfaces exposed to the plasma are DPP electrode materials (e.g., copper, silver, or additives) and the insulators (e.g., refractive ceramics AlN, Al_2O_3, and BeO).[94] Because of the high-energy transfer density over the small electrode, excellent conductivity is critical for preventing evaporation and electrode overheating.

A 2005 publication reported that a DPP EUV source produced 200 W EUV radiation at 2π sr solid angle and IF power of 25.7 W (CE=1.0%) using xenon fuel and 400 W/2π (CE=2.0%), corresponding to 51.4 IF power using tin fuel.[95] In 2006, it was reported that the capability of reaching 800 W in 2π sr from a tin DPP EUV source in burst operation, corresponding to 70–120 W IF power, but the required duty cycle and electrode lifetimes may not be met by using this standing electrode design *Z*-pinch approach.[96] A new rotating disk electrode is being designed to overcome these limitations.

By 2007, DPP EUV source has the capability of 702 W power with conversion efficiency of 1.2% in 2π sr solid angle and 2% bandwidth using tin fuel, which correspond to 55–62 W EUV power at intermediate focus with estimated electrode lifetime of about one week.[97]

However, the high heat load on small electrode makes the electrode material consumption inevitable. This common phenomenon of high-temperature plasma electrode may be the most challenge for DPP application as EUV light source. The lifetime of electrode then is a critical challenge. The high heat load also affects the lifetime of collector optics. The EUV source power at intermediate focus may be not as challenging as the lifetime of electrode and collector optics. Because these disadvantages are intrinsic on this method, it is extremely difficult to overcome it.

LPP was proposed as an EUV source in the first EUVL publication in 1988 and was used as a source in ETS tool later. The primary challenge is to obtain a high laser power of 10 kW and pulse repetition rates of several kilohertz. Maintaining a high laser repetition rate is important for obtaining high EUV in-band power. Short laser pulses and high repetition rates tend to result in high conversion efficiency.

High CE requires a fresh surface for the laser target, which makes movable targets preferable such as liquid-jet and microscopic liquid droplets. A liquid-jet LPP EUV source gained much attention as an EUVL source, but it has the disadvantage of high liquid volume. Therefore, liquid droplet with accurate control and integration of laser may be the best choice.

LPP obtained very promising progress recently. In 2004, 7 W EUV in-band power was obtained in a 2π sr solid angle using 0.7 kW laser power on a xenon-jet target, corresponding to IF power of 2.3 W and CE of 1%.[70] By 2005, a LPP EUV source using 1.2 kW laser power and a xenon target produced 10 W EUV power at 2% bandwidth, and 3.3 W IF power with CE of 1%.[95]

In 2007 SEMICON West, Cymer announced a significant progress of their LPP source and obtained EUV power of 50 W at intermediate focus, with 6 kW laser and tin droplet target, by using a short pulse, high power CO_2 laser. It is expected to obtain 100 W EUV IF power with 10 kW laser by the end of 2007. When this target is attained, the industry will almost meet volume production requirement for 5 mJ/cm^2 resist and 100 wafers/h. The collector lifetime is estimated to be one year by using this LPP source.[98] If the laser has acceptable stability and lifetime, LPP may become the leading candidate of EUV source again.

IV. MULTILAYER COATING

EUV reflective optics require a reflective mirror, i.e., a suitable multilayer coating to reflect EUV light at or close to normal incidence or, with smooth metal reflectors, at grazing incidence angles.

A multilayer reflecting mirror with a broad wavelength band for EUV and soft x ray was used for telescopes in space science before being applied in EUVL. The multilayer coating in EUVL is a very narrow-band, resonance-reflecting mirror on the lithography tool camera and illumination condenser. Although specifications for these two applications differ in some respects, basic requirements are stable high reflectivity, long lifetime, and uniform properties. The multilayer material consists of repeated bilayer pairs; the relationship among the bilayer space, d, incidence angle, θ, and wavelength, λ, is expressed as

$$n\lambda = 2d \cos \theta. \tag{3}$$

For 13.5 nm wavelength EUV radiation, space d (i.e., the bilayer thickness with maximum reflectivity) is 6.79 nm with a 6° incidence angle, and the 40-pair multilayer thickness is 271.5 nm. The most common multilayer mirror consists of 40 Mo/Si layer pairs.[99,100] The multilayer number depends on the disparity in indices between materials. Currently available materials have the order of 10^{-2}, resulting in multilayer stacks up to 40 layer pairs.[101]

To reflect EUV radiation on a bilayer structure, we need a high-electron-density material (absorber), e.g. metal, and a low-density-electron material (spacer), e.g., semiconductor, as a pair.[1] The following are the typical absorber/spacer material pairs and their lower limits of working wavelength: Sc/Si (36 nm), Mo/Si (12.5 nm), Mo/Be (11.4 nm), Ru/B_4C (6.7 nm), Co/C (4.4 nm), Cr/Sc (3.2 nm), and W/Si (0.7 nm).

Based on the emission spectra of EUV light, the focus is on two wavelengths, 13.5 and 11.4 nm, corresponding to Mo/Si and Mo/Be multilayers. The main consideration in choosing between these two includes the throughput of the optical system, the wavelength mismatch, and the sensitivity of the resist, as well as environmental and health hazard.[102] According to these criteria, Mo/Si was selected by the industry as the main EUV multilayer structure.

An important requirement for the multilayer used for the condenser is thermal stability, especially on the first multilayer mirror without mitigation system. The high heat load can cause interdiffusion, change the *d*-space thickness, and shift the peak reflectance wavelength. It was reported that in an 8th exposure to a xenon discharge source, 18% reflectivity may be lost.[103] The fundamental requirement for the condenser is to collect and transport sufficient in-band EUV radiation with uniform illumination on the EUV mask. In early EUVL studies, 11% condenser transport efficiency was obtained, which was close to the theoretical maximum values, leaving lifetime as the remaining challenge.[15] When the multilayer is exposed to a high temperature, the chemical potential difference of the two layers can cause interdiffusion at the boundary of the multilayer pair, resulting in the thickness change of the individual layers. Therefore, interdiffusion prevention and stress control are essential in multilayer coatings. Compound multilayer and diffusion barriers are commonly used to increase thermal stability, but may diminish reflectivity.

Both direct current (dc) and radio frequency (rf) magnetron sputtering deposition can be used to produce the multilayer. However, these methods create an intrinsic issue and challenge—periodic stress between layers in the multilayer structure. Its transfer from compressive to tensile in the Mo/Si multilayer was observed.[27] Stress should be controlled to minimize the stress-induced deformation. It does not depend on the number of the bilayer pairs, but on the ratio of the layer thicknesses. For a film on a substrate, the film stress, σ_f, can be expressed by the Stoney formula[104,105]

$$\sigma_f = \frac{1}{6R}\frac{E_s d_s^2}{(1-\nu_s)d_f}, \tag{4}$$

where E_s is the substrate's Young's modulus; d_f and d_s are the film and substrate thicknesses, respectively; R the radius of curvature; and υ_s Poisson's ratio. Annealing is very common for reducing the intrinsic stress on the multilayer, but it may cause reflectivity loss. Electron beam evaporation with low-energy ion-beam smoothing was reported to reduce multilayer induced stress from normally −180 MPa to less than −30 MPa using a mitigation method without scarifying reflectance, with reflectivity of 68%–69%, near the theoretical values.[106]

Replacing the original Mo layer with a trilayer of Mo/Ru/Mo can significantly change the stress from compressive stress of −450 MPa to tensile stress of +14 MPa without significant changes in reflectivity and bandwidth by using ion-beam polishing[107] or ion-beam sputtering.[108] The gas composition in the sputtering chamber plays an important role in multilayer stress. When oxygen gas was introduced, the stress change after the deposition of the subsequent silicon layer was almost zero, resulting in low stress. However, when nitrogen gas was introduced and only pure argon gas was used for IBP, the subsequent silicon layers exhibited compressive stress changes.[109] These results indicate that the molybdenum oxide formation contributed to stress reduction. It was also reported that multilayer sputtered by low-pressure rotary magnet cathode sputtering with xenon gas produced higher reflectivity than when argon gas was used, and that the multilayers sputtered at a lower pressure exhibited higher reflectivity than those sputtered at a higher pressure.[110]

The layer thickness changes were observed when the multilayer was annealed at a temperature higher than 400 °C.[43] Crystallization may occur and reflectivity loss may result from formation of an interlayer.

Interdiffusion at the interface of two materials is a common transport phenomenon. Diffusion in solid phase generally has a very low diffusivity, but for diffusion in thin film with thickness of 2–5 nm, the diffusivity may be significantly high. The diffusion in solid is an overall result of diffusions in lattice, grain boundary, and dislocation. Among these three mechanisms, diffusion in grain boundary plays an important role. To prevent interdiffusion between two thin films, a diffusion barrier is a common method. It sandwiches between the two layers. It should not significantly affect optical properties, but should have small diffusivity of silicon and molybdenum and thermodynamic stability, as well as good adhesion. Besides, a stable eutectic compound with high melting point in the two-element pair may decrease the diffusion rate, but the eutectic alloy may be formed. Unfortunately, the Mo/Si multilayer has a large solid solution area, which makes it vulnerable to interdiffusion. The reflectivity and layer structure can be affected by annealing at a temperature higher than 400 °C.[43] It was reported that the thermally induced deteriorations of the Mo/SiC, Mo/C, Mo/B_4C, Mo/BN, $MoSi_2$/Si, and Mo_5Si_3/Si multilayers are smaller than those of the Mo/Si multilayer. However, the Mo/Si layer has the highest EUV reflectivity and compromises may be made in multilayer selection. Boron carbide diffusion barrier between molybdenum and silicon can significantly reduce silicide formation at the interface; for example, a 0.4 nm thick boron carbide for the Mo-on-Si interface and a 0.25 nm thick boron carbide layer for the Si-on-Mo interface produce the best results, with 70% reflectance at 13.5 nm.[99] Mo_2C diffusion barrier also significantly improves Mo/Si multilayer thermal stability up to 600 °C, but at the price of low reflectance (59.9%).[111]

The Mo/Si multilayer structure was studied and characterized using x-ray diffraction, x-ray reflection, transmission electron microscopy, selected area electron diffraction, and Rutherford backscattering spectroscopy spectra, showing the presence of a mixed Mo–Si layer between Mo and Si interfaces.[112]

Kinetics of intermixing in the Mo/SiC multilayer was studied. The proposed composition of the interlayer was $Mo_\beta(SiC)_{1-\beta}$ with the rate equation[113]

$$\frac{dw}{dt} = \frac{D(T)}{\beta(1-\beta)w}, \tag{5}$$

where w is the mass of the interlayer, and $D(T)$ is the temperature-dependent interdiffusion coefficient, which can be expressed as

$$D(T) = D_0 e^{-E_A/kT}, \tag{6}$$

where E_A is interdiffusion activation energy, D_0 is constant, k is Boltzmann's constant, and T is temperature. The above kinetic equation shows interlayer formation is enhanced at higher temperatures.

When the multilayer is exposed to ambient conditions, the top Mo layer can be oxidized, resulting in scattering and lower reflectivity. Therefore, a protective silicon or carbon layer can be used to prevent the top metal layer from oxidizing in atmospheric oxygen (i.e., the silicon or carbon capping layer on top of the Mo layer[28] or ruthenium capping layer[99]). A boron carbide layer was also used as a diffusion barrier between a ruthenium capping layer and the top silicon layer. A Ru-on-B_4C-on-Si layer was used as a multilayer capping layer and found to have a lifetime 40 times longer than Si-capped multilayer optics.[114] Compared with this capping layer, the lifetime of a ruthenium-capped multilayer may be too short to be used in commercial tools. Therefore, RuO_2 was proposed as a capping layer.[115]

Smoothing of the layers and contamination control are major challenges in the multilayer coating process. Ion-assisted polishing of multilayer coatings is a common technology.[106,116] However, sub-nanometer-sized particles on the substrate to be coated with Mo/Si may nucleate critical phase defects in the coating, significantly degrading its optical performance and reducing device yield.[116–118]

Degradation is a critical challenge when the multilayer was exposed to EUV light. Reflectance was reduced through oxidation of the top silicon layer on the Mo/Si multilayer and carbon formation on the mirror, mainly by the dissociation of absorbed hydrocarbon. The reflectance loss of the single multilayer mirror should be 1% or less over its lifetime, which corresponds to a 10% energy loss total for a ten-mirror stepper.

Optics and camera performance characterization includes profilometry, atomic force microscopy, EUV reflectometry, and EUV scattering.[119] E-beam based deposition obtained an added-figure error of 0.02 nm,[120] (i.e., the subatomic distance range) or even 0.015 nm in EUVL multilayer coatings.[121] Comparison of Mo/Si multilayer coatings deposited by ion beam and magnetron sputtering showed reflectance of 62% and 65%, respectively.[122] The interface layer thickness sputtered by ion-beam sputtering was 30%–50% thicker than that formed by magnetron sputtering.

Defect characterization is yet another challenge associated with EUV multilayer coating. At-wavelength (i.e., using the same wavelength as exposure tool) defect characterization was developed for this purpose.[123] Basic requirements on protection capping layer is high and stable transmission, chemical resistance (e.g., oxidation), and suppression of oxygen and hydrogen permeation into the multilayer system.[115] Very small changes on transmission in capping layer can cause significantly overall reduction of EUV reflectivity due to the multiple mirrors (e.g., ten mirrors) in optical system. Although mitigation system has significant progress, very small amount chemicals can cause damage on the capping layer with thickness of 1–2 nm. EUV light has so high photon energy that it dissociates gaseous oxygen containing chemicals to form atomic oxygen, which can oxidize capping layer materials such as silicon or ruthenium. Therefore, ruthenium oxide may be a more suitable capping layer material with some trade-off on transmission. Permeation of hydrogen and oxygen in the thin capping layer is a challenge. The practical multilayer composition and lifetime will be finalized only after long-term exposure data become available.

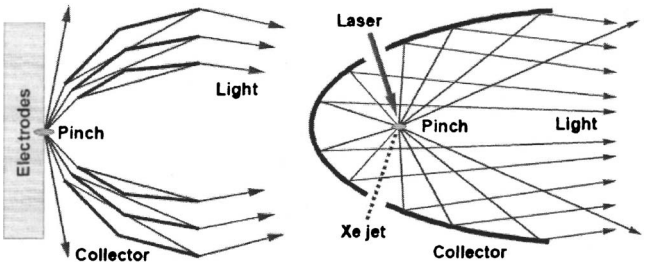

FIG. 6. Schematics for EUV collect optics of discharge produced plasma (left) and laser-produced plasma sources (right).

In summary, main challenges of multilayer lie in the multilayer properties such as thickness and uniformity, lifetime, and defectivity control. Multilayer is used in collector lenses, projection optical lenses, and masks. For the multilayer on collector optics, lifetime and stability are the most challenging, while the multilayer on masks has a very strict specification on defectivity control.

V. OPTICS AND METROLOGY

A. Optics

EUVL optics consists of illumination (condenser) and projection optics, the former for efficient EUV light collection to illuminate a mask plane, and the latter to image the mask pattern onto the wafer. Field uniformity is a basic requirement for the illuminator. The main illumination condensers include Kohler and critical illumination condensers. Given the uniformity requirement, the Kohler illuminator or critical-Kohler condenser is preferred for full-field exposure tools.[124] Figures 6 and 7 show schematics of condenser optics[125] and EUV lithographic camera.[51] The condenser design is dependent on the type and configuration of the EUV light source; hence, final condenser design will be determined by ongoing developments in EUV source technology.

Due to the limited EUV source power, EUV collector optics need to collect as much EUV in-band power as possible. Using a condenser optical system is a traditional optical ap-

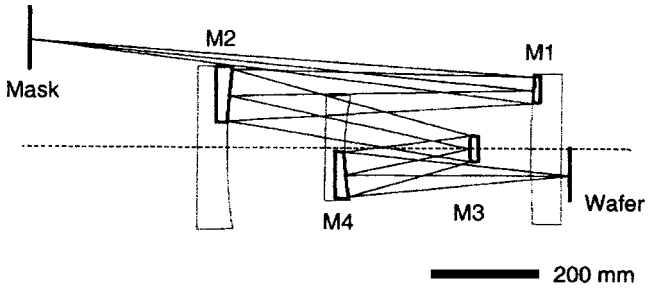

FIG. 7. Schematic of the ETS EUV lithographic camera.

proach; however, the real challenge of the EUV condenser lies in the prevention or removal of contamination created during EUV exposure. Erosion of multilayer condenser optics by the EUV source plasma is significant, with higher EUV intensity resulting in higher erosion rates.[52,126] For a production tool, 30 000 h of exposure time is required.[127]

A DPP EUV source using tin fuel is a promising EUV source candidate. However, condensation of a very thin layer of tin (e.g., 2 nm) can reduce reflectance by as much as 20%.[128] Besides this condensation, energetic charged particles result in sputtering and implantation, causing surface roughness and reflectance reduction. A gas curtain for debris mitigation is applied for controlling this type of contamination.[128,129] Due to the very high power (e.g., 50–70 kW) and plasma discharge applied very close to condenser, the discharge plasma will inevitably affect the lifetime of condenser lenses and discharge electrode, which significantly affect the application of this EUV source. Compared with DPP, LPP laser source is far away from condenser, preventing too high temperature environment near the condenser optics. Therefore, the progress in LPP source is very helpful for improving the lifetime of condenser and debris mitigation.

EUV absorption on the condenser mirror changes the temperature of the mirror and, consequently, unstable reflectance. A high-temperature collector mirror with a working temperature of 400–500 °C and adjustable capability may keep the mirror temperature stable,[130,131] but high temperature may result in interdiffusion of multilayer and then the reduction of reflectance.

Collector dimension is critical to illumination optics. Large size favors solid angle, debris mitigation, and long lifetime, but makes fabrication difficult. A 320 mm diameter ellipsoidal collector coated with a graded multilayer and 1.6 sr solid angle was reported.[131]

In the EUVL projection optical system, the optical properties are limited by aberration and diffraction. Even for an aberration-free, partially coherent aerial image, diffraction effects still result in adjacent bright image features interfering with each other, i.e., "proximity effects." One of the main reasons for using short wavelength EUV light is to control proximity effects. It is a major challenge to image over a large field at the diffraction limit. Scanning ring-field lithographic projection optics over a narrow annulus is effective and practical in controlling aberration. EUVL optical systems require high image contrast over the full-field range with an extremely low distortion over the entire field.

To reduce aberration, multiple mirrors are usually used for lithographic optics, but they significantly increase the difficulty of fabricating and testing the substrate. WFE requirements for diffraction-limited imaging scale with wavelength. When wavelength changes from 193 nm ArF to 13.5 nm EUV, about 14× smaller allowable WFE for EUVL system is required. Therefore, for a four-mirror system with an allowable surface figure error being one-half of the WFE based on Marechal's wave front error criterion of $\lambda/14$, the allowable average figure error is 0.56 nm rms deviation from a perfect sphere. Table IV shows specifications for surface figure error as well as mid-spatial frequency roughness (MSFR) and high-spatial frequency roughness (HSFR) for scattering control.[132] Figure error plays an important role in determining aberration, while MSFR and HSFR are critical to image contrast and EUV intensity, respectively.

The optical systems on ETS and AD tools have ring-shape full-field sizes of 24×32.5 and 26×33 mm^2, respectively; the former uses four-mirror optics with a NA of 0.1; the latter uses six-mirror optics with a NA of 0.15–0.25. It is expected that an eight-mirror system will be used to improve optical properties in the future. It is clear that a high NA can be obtained by using six mirrors instead of four. The challenge for EUV optical fabrication is to simultaneously meet the specifications for figure errors and roughness on aspherical surfaces.

EUVL optics is close to meeting specification. Flare has been the subject of several intensive studies recently.[133–139] It depends on mirror quality, but also on feature size; sometimes it can be as high as 40%.[140] This means that flare in an EUVL system is dependent on IC layouts and flare correction techniques may be needed.[140] In EUVL, a contrast transfer function, i.e., the measure of the aerial image contrast as a function of pitch, was observed and should be considered.[141]

TABLE IV. Nominal specifications for EUVL projection optics (six-mirror system).

Error term	Maximum error specification	Optical properties by 2007[a]
Figure error, nm rms	0.08 nm rms	0.05 nm rms
Mid-spatial frequency roughness (MSFR), nm rms	0.14 nm rms	0.15
High-spatial frequency roughness (HSFR), nm rms	0.10 nm rms	0.09

[a]References 45 and 132.

Flare results from surface roughness, especially the mid-spatial frequency roughness from 1/mm to 1/μm. It is inversely proportional to the square of the wavelength.[138] EUV flare can be predicted based on the surface roughness of the individual mirrors and then can be corrected in the mask design.[134,138]

For future EUVL production exposure tools, the target is to control flare within 8%, which corresponds to a projected optic MSFR level of $\leqslant$0.14 nm rms.[56] This level of MSFR is feasible based on current optimized test mirror data.

Capping layer oxidation and carbon deposition occur on EUV optics. The control of capping layer oxidation relies on capping material, while the deposited carbon can be cleaned by atomic oxygen or hydrogen.[142–145] However, much more data on continuous high-power operation are needed for accurate evaluation of stability and damage of EUV optics.

B. Metrology

The basic requirements of metrology for EUVL are accuracy, precision, and practicality. EUVL metrology consists primarily of optical system characterization for fabrication and optical property changes caused by EUV radiation. The accuracy and precision of the optical figures was a major challenge to metrology and fabrication technologies during early work on EUVL. Because phase errors cannot be detected by visible-light interferometry, at-wavelength interferometric testing is a necessary metrology method in developing EUVL optics. It is used mainly for wave front measurement, and final testing and alignment to adjust and minimize cumulative errors. Another important metrology application for EUVL is the measurement of reflectance of the multilayer on the EUV mirror and mask. To characterize the aberrations, interferometry with subnanometer wave front measuring accuracy is necessary.

The lack of long-coherence-length light sources at EUV wavelengths makes it very difficult to characterize EUV optical systems. Therefore, common-path techniques became the basic method for at-wavelength wave front characterization, including point diffraction interferometry and shearing interferometry. The EUV wave front is produced by figure of mirror surfaces and by multilayer coating properties.[146,147]

Two categories of errors are present in an optical system, statistical errors and systematic errors. The former includes repeatability and reproducibility, while the latter includes rotational symmetric errors. Both must be characterized to an acceptable level using metrology techniques.

Diffraction-limited imaging is preferred for EUVL. Based on the Marechal criterion, the WFE W_{EP} of the imaging wave front in the exit pupil of the imaging system should follow,[148]

$$W_{\mathrm{EP}} \leqslant \frac{\lambda}{14} \quad (\mathrm{rms}), \tag{7}$$

where wavelength λ is 13.5 nm.

EUV metrology methods include phase-shifting point diffraction interferometry,[146] line diffraction interferometry, phase-shifting lateral shearing interferometry, slit-type lateral shearing interferometry, digital Talbot interferometry,[149] cross-grating lateral shearing interferometry, and double-grating lateral shearing interferometry. Among all these methods, point diffraction interferometry has the highest accuracy and precision. However, for a high-NA projection optical system, a very small pinhole is needed for producing an ideal spherical wave front used as a reference wave front, and EUV intensity drops, i.e., a stronger EUV light is needed.

For the diffraction limit, each aspheric mirror on a six-mirror projection camera should have absolute figure accuracy approaching 100 pm rms.[150] By 2002, an absolute accuracy of 250 pm rms on a visible-light phase-shifting diffraction interferometry was obtained.[150] By using at-wavelength, EUV interferometry accuracy levels of 41 pm for 0.08 NA measurement and 67 pm for 0.1 NA were reported.[151] These results show that the critical challenge of EUV optical characterization was overcome.

Reflectometry is an important aspect of metrology for the multilayer coatings of optics and masks for EUVL and recently reflectance measurement has been receiving more attention. Many research works were reported for improving the EUV reflectance measurement.[152–155] Unlike optical characterization by interferometry, reflectance measurement by reflectometry is not very challenging, but optics dimensions may not be suitable. It was reported that at NIST an EUV reflectometry facility with a large chamber that can hold optics up to 36 cm in diameter was installed and that, after modification, it will accommodate optics up to 50 cm in diameter.

Currently, EUVL is studied and developed in three main areas: the United States, Asia, and Europe. The agreement of accurate reflectance is important. A cross-calibration EUV reflectance measurement was made between the Physikalisch-Technische Bundesanstalt at BESSY II, which serves the European EUVL program, and the Center for X-ray Optics at the Advanced Light Source, which serves the United States EUVL program.[153] Agreement within the mutual relative uncertainties of 0.14% for reflectance and 0.014% for wavelength was obtained.

VI. RESIST

Resist is one of the most challenging issues for next-generation lithography technology. The basic requirements for lithographic photoresist are sensitivity, resolution, linewidth roughness or line edge roughness (LER), outgassing, EUV absorption, pattern cross-sectional aspect ratio and profile, pattern transfer and etch resistance, defect density, and reproducibility. Among them, the sensitivity, resolution, and LER are the most challenging. Outgassing can contaminate the projection optics and reduce the lifetime of the optics in the EUVL exposure tool. Today's state-of-the-art resist is chemically amplified resist (CAR), which is widely used for 248 and 193 nm optical lithography. The main advantage of CAR is its high sensitivity and resolution. However, its drawbacks for EUVL are LER and pattern collapse, as well as absorption of the EUV light, which affect the resolution

and cross-sectional profile. LER does not scale down with the shrinking critical dimension (CD) feature sizes. Therefore, LER reduction and control is one of the biggest challenges for next-generation lithography. For practical EUVL application, LER should be controlled below 2 nm (3σ).[156–158] In the non-CAR EUVL resist group, PMMA is the main candidate.

CAR properties are dependent mainly on photoacid generator (PAG) and polymer types, the former including silicon-containing acrylic MA type, POSS, PHOST, Fujitsu, and ESCAP, and the latter including TPS-R type, DPJ type, BTHT type, and phthalimide type. The power limit of the EUV source necessitates a low exposure dose, likely below 10 mJ/cm^2. This also requires high PAG loading and high sensitivity. For 32 nm node, resist thickness of 55–100 nm is required to meet aspect ratio controls on small features. Meanwhile, the thin resist requires a high etch resistance during pattern transfer. To date, CARs with sensitivity of 2–10 mJ/cm^2 are common in EUVL studies.

Resist resolution is strongly affected by pattern collapse, which becomes increasingly important as feature sizes approach those for EUVL. CD resolution and LER are challenges not only for EUVL resist, but for all next-generation lithography resists. The pattern collapse mechanism has been intensively studied.[159–161] It occurs when physical properties of the materials cannot withstand the capillary force during the drying of the rinse liquid.[162–167] Pattern collapse depends on the pattern height or aspect ratio. The critical aspect ratio, at which patterns begin to collapse, is expected to be larger than 3 for EUVL,[159,166] but currently for features less than 50 nm, the critical aspect ratio is approximately 2 or less. The current approach to improve it includes surfactant rinses,[168,169] bilayer resist technologies,[163,170] and supercritical CO_2 dryers.[164,165] The main advantages of supercritical CO_2 are low viscosity, zero surface tension, and tunable density. It was reported that resists processed in supercritical CO_2 solutions using CO_2-compatible salts (CCSs) substantially reduced pattern collapse and obtained dense line/space features with aspect ratios greater than 12.[171] The features developed using the CCS process also have substantially lower LER than those developed by TMAH.[171–173]

Outgassing is another challenge, which arises mainly from byproducts of the polymer deportation reaction and PAG decomposition of the CAR, as well as small molecular weight additives and solvents. The high-vacuum environment required by EUVL also enhances outgassing. Therefore the challenge of EUVL resist is to improve sensitivity and minimize outgassing simultaneously, but there is a conflict between resist sensitivity and outgassing, i.e., highly sensitive PAG generates more decomposed products. The International Technology Roadmap for Semiconductor 2006 Update specified an outgassing rate of 5×10^{13} molecules/cm^2 s. So far, many commercially available resists can meet this specification, but the practical outgassing requirement may be much stricter than the ITRS standard. Resist with high activation energy and nonionic PAGs may produce less outgassing.[174] As of spring of 2007, outgassing control for EUVL CAR was reported at below the detection limit of gas chromatography-mass spectrometry (GC-MS), i.e., less than 1×10^{10} molecules/cm^2 s.[175]

TABLE V. Atom absorbance.

Atoms	Absorbance
H	1
Si	13.6
C	23.8
N	49.6
O	93.4
F	141

LER is a very difficult challenge for EUVL resist. The mechanism that causes it is very complicated. It was reported that small PAG size and high PAG concentrations have low LER, and high quencher concentrations at good aerial image contrast also reduce LER.[176] Postexposure bake is also a significant contributor.

With the shortening of exposure wavelength, photon energy increases from 5 eV at 248 nm to 6 eV at 193 nm and then to 93 eV at 13 nm, of which discrete photons may be responsible for the LER.[177] For the same exposure energy, high individual photon energy has a smaller number of photons per pixel, resulting in a shot noise and LER. One approach to control LER is to use an ultrathin single-layer resist over a hardmask.[178] It was reported that shot noise was observed at deep ultraviolet (DUV) and EUV for seven examined resists; LER follows Poisson statistical rules, i.e., it is inversely proportional to the square root of the dose.[179]

EUVL resist is also prone to sidewall issues as a result of EUV light absorption and then absorbance reduction for EUVL resist obtained intensive studies.[170,180–182] Inorganic resists containing highly transparent silicon atoms and ultrathin resist or bilayer EUVL resist shows advantages. 20 nm features with an aspect ratio of 10:1 were obtained on bilayer resist layer (200 nm thick), but pinhole formation may be a challenge.[170]

The mechanism of EUV light absorption differs from that of optical resists. The overall absorption of EUV is the total result of the atomic absorption in a molecule. A pattern in the thin layer can be generated by EUV exposure and then transferred through the remaining resist thickness, usually by using an anisotropic oxygen plasma etch.[183]

As shown in Table V, atoms of oxygen and fluorine have high absorbance, while atoms of carbon, hydrogen, and silicon have low absorbance.[184] Therefore, silicon backbone polymers were preferred for absorption reduction.[182] It was reported that boron atoms in EUVL resist can lower EUV absorption[185] and improve etch resistance.[181,186,187] Calculated optical density of resist was found to be 4.0 μm^{-1} (base e), corresponding to transmittances of 67.0% and 44.9% for 100 and 200 nm resist thickness, respectively, and 120 ± 15 nm imaging layer thickness was suggested.[188]

It was reported in 2005 that Intel EUVL resist development was close to meeting their 32 nm technology node tar-

TABLE VI. Intel EUVL resist requirement for 32 and 22 nm technology nodes (Ref. 189).

Properties	Requirement
Resolution	32 and 22
Depth of focus (DOF)	$\geqslant 0.2\ \mu$m
LER (3sigma)	<1.5 nm
Photosensitivity	$2-5$ mJ/cm^2
Outgassing	$10^{10}-10^{11}$ molecules/cm^2
Sidewall angle	$(90\pm2)^\circ$

get shown in Table VI,[189] except for LER. Some correlation exists among the resist parameters, making it very challenging to meet all specifications simultaneously. One example is that sensitivity and LER compete with each other.

Figure 8 shows a top view of resist pattern exposed by EUV.[190] Recent results on EUVL resist presented at the 2007 SPIE Advanced Lithography conference show significant progress.[175,191,192] Although further optimization and progress are needed, EUVL resist now is not a "show stopper." In fact, 25 nm 1:1 line:space feature resolution with EUV lithography was obtained on a novel CAR called XP6627,[193] with a low LER of 2.7 nm 3σ. These properties demonstrate substantial progress in EUVL CAR and raise the possibility of extending CAR to the 22 nm node. Other CARs having new anionic PAGs and corresponding polymers showed improved sub-50 nm resolution, with 50 nm 1:1 and 20 nm 1:4 line:space obtained.[191] Contact holes are a very challenging pattern for lithography. By 2006, contact holes of 50–150 nm were also reported.[194]

Molecular resists for EUVL also made significant progress by 2007 in terms of sensitivity and LER.[192] Results showed sub-45 nm patterns at an exposure dose of 12 mJ/cm^2 and LER values of 3.1 nm.

In summary, EUVL resist has made significant progress in the last few years, especially after 2000 when small-field EUVL exposure became available. While it is closer to the final target of EUVL on the sensitivity, resolution, and LER, the main challenge is to satisfy all three requirements simultaneously.

VII. MASK

Presently, developing a suitable quality EUVL mask is the top challenge in the whole EUVL program. EUVL mask technologies consist of EUVL blank mask preparation and mask fabrication from raw stock. The blank mask preparation requires flat and defect-free substrate with an extremely low coefficient of thermal expansion (CTE), defect-free multilayer with accurate thickness and chemical composition, and a suitable characterization method to ensure quality. Mask fabrication from raw stock includes pattern generation, pattern transfer, metrology quality control, and defectivity control. It was reported that Intel established an EUV mask pilot line for implementing EUVL technology.[195]

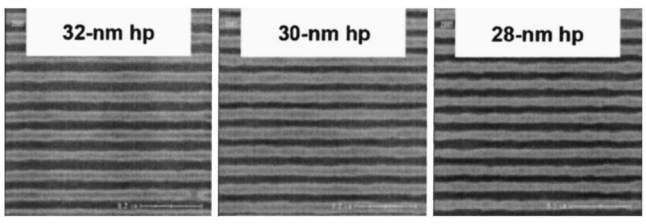

FIG. 8. Top-review resist pattern.

In the 1990s, EUVL was expected to be implemented at 100 nm, but now it is anticipated for 32 and 22 nm nodes. Phase shift masks for EUVL were studied for higher resolution by etching of a multilayer reflector to about 100 nm depth.[196–200] However, it is too early now to get any conclusion on EUV phase shift mask feasibility.

EUVL masks have a reflectance of 65%–70%, i.e., the rest of the EUV energy is absorbed by the mask, mainly the substrate, due to its large volume compared with the layers. This absorption causes thermal expansion, which must be strictly controlled to remain within overlay error budgets. Therefore, near-zero thermal expansion materials with CTE less than 5 ppb (as parts per 10^9)/K are required for 32 nm node.

EUVL mask substrates must be extremely even to avoiding shifting the pattern through out-of-plane displacement (OPD) and global height variation that results from OPD.[201] Defect requirements depend on the technology node. At the originally planned 100 nm node, the requirement was zero defects greater than 80 nm polystyrene latex (PSL) equivalent size. However, the defect specification for the 32 nm node is 26 nm PSL equivalent size.

The optical mask substrate in current usage is fused silica with a CTE of 500 ppb/K. This value does not meet the requirement for an EUVL mask substrate. Ti-doped and Sn-doped silica glasses may have lower CTE than fused silica.[202] CTEs of 0 ± 5 ppb/K (Ref. 202) for Ti-doped SiO_2 glass and 0 ± 30 ppb/K for SiO_2–TiO_2 binary glass[203] were reported. However, compositional striations were found in low-CTE glass that may affect surface roughness when the glass is polished.[203] To date, CTE can meet 0 ± 12 ppb/K in the temperature range of 12–25 °C, and $\leqslant 7$ ppb/K at any single temperature.[204]

The first challenge in EUVL mask fabrication is the preparation of raw stock. It is very complicated to manufacture acceptable-quality multilayer for EUVL masks. Reflectivity, thickness uniformity, and defectivity controls are the main issues. EUVL masks require not only substrate flatness on the front side no more than 32 nm peak-to-valley (p-v) for 32 nm node, but also the same value on the back side to ensure appropriate contact with the electrostatic chuck. Current goal of flatness in 2007 is 50 nm p-v.[205] Substrate with best integrated performance has 120 nm p-v front on the front side and 198 nm p-v on the back side. The printability of buried defects in multilayer is also dependent on the relative multilayer position.[206] Generally speaking, substrate or phase defects are considered nonrepairable, because they lie underneath or are embedded in the multilayer.

Before 2000, EUVL masks for 100 nm technology required fewer than $0.01/cm^2$ defects at a detection threshold of 50–80 nm.[207,208] At that time, detection of $0.1/cm^2$ for defects larger than 130 nm employed visible light inspection tools.[208] By 2002, the EUVL application technology node had been pushed out to 65 nm and defect density of 0.0025 printable defects/cm^2 for both the mask substrate and the multilayer was required to obtain a mask blank yield of 60%.[209] The coating technology also made progress with defect levels of $0.05/cm^2$ for defects greater than 90 nm PSL.

By 2004, EUVL was targeted for the 45 or 32 nm node, and the defect control on the blank mask became stricter. Actinic defect inspection could detect defects of 70 nm wide and 3.5 nm high.[211] In the following year, the mean multilayer-coating-added defect density attained 0.055 defects/cm^2 for particles greater than 80 nm in size (PSL equivalent) with best results of 0.005 defects/cm^2.[211]

To prevent defects within the multilayer stack from printing on the wafer, EUV mask blanks must have "0" defects, i.e., a defect density less than $0.003/cm^2$ at greater than 25 nm for the 32 nm node,[212] based on the critical defect size of 80% half-pitch technology node. Therefore, for the 22 nm node, the defect dimension should be controlled at 18 nm on the mask. We still have challenges in developing defect inspection, repair, and effective control on mask blanks.

Multilayer defects are phase defects. They locally change the reflective property of the multilayer by changing the phase or amplitude. Production cost and complexity dictate that EUVL mask blanks be inspected and repaired. Both raw material and pattern inspections are necessary. The former includes substrate and multilayer inspections; the latter is similar to that for optical mask. Both DUV light (nonactinic)[213–215] and at-wavelength light (actinic)[216–219] are used in carrying out inspections.

Multibeam confocal inspection, a nonactinic method, is generally regarded as a very promising method for mask blanks[215,216,220–222] and is the main inspection of EUVL mask to date. It still uses deep ultraviolet (e.g., 257 nm wavelength), which was designed for KrF wavelength (248 nm) and extended to ArF mask. Although some investigators assert that actinic inspection may not be necessary,[223] at-wavelength inspection will likely emerge as the final solution for EUVL mask. Till now, inspection tool using 266 nm wavelength has the inspection capability of 41 and 52 nm PSL equivalent sizes on quartz and multilayer surface, respectively.

For high-sensitivity inspection, actinic detection of multilayer defects in EUVL mask blanks was studied,[224–226] showing a better sensitivity[210,227] than the state-of-the-art nonactinic mask blank inspection system. In 2004, it was reported that defects of 10–12 nm high and 50–65 nm wide could be detected with a greater than 90% capture rate.[215]

By 2006, buried defects of 30–50 nm as well as a phase structure of 6 nm high could be detected by actinic mask blank inspection using photoelectron emission microscopy.[226] However, simulation studies showed that an 80 nm phase defect 3 nm high might be printable.[196,226] Simulation results also showed that CD change increased linearly with the height of a phase defect, but nonlinearly with that of an amplitude defect.[228] The reason that defect height is the factor determining printability is the disruption of constructive interference of the reflections on each of the multilayer interfaces.[221]

Creating a nonpellicle EUVL mask is a major obstacle. To overcome this challenge, thermophoretic protection obtained investigations.[223,229–231] Two basic requirements for thermophoretic protection are that the mask be kept warmer than its surroundings and that the surrounding pressure be sufficiently high to enable thermophoretic protection. Fortunately, EUV absorption naturally results in the mask being warmer than its surroundings. Robust thermophoretic protection was observed over argon gas pressures of 50–1600 mTorr, particle size of 65–300 nm, and temperature gradients of 2–15 K/cm.[231] Use of a movable pellicle[232,233] and a wire-mesh-based nonmovable pellicle with very thin ruthenium or silicon film were reported, but results were unsatisfactory.

Absorber on EUVL is another challenge. The basic requirements for the absorber layer are high reflectance contrast, thin layer thickness, and adequate extinction coefficient. Absorber materials with high extinction coefficient enable use of a thin film to reduce the influence of off-axis incidence. In early EUVL studies, a chromium-based absorber was used because it was readily adopted from binary optical masks.[234–238] Tantalum-based absorber materials, such as TaBN, TaGeN, and TaSi; were adopted from proximity x-ray lithography.[239–243] When TaBN is used as an EUVL absorber, TaBO is the antireflective coating material. Studies on tantalum-based EUVL absorbers are focused on TaN,[244–247] TaBN,[248–250] TaGeN,[251] and TaSi.[252] A proposed combined absorber stack for EUVL masks consists of Al_2O_3 as the antireflective portion and TaN as the bulk portion.[253] The significant advantage of this configuration is the thinness (47 nm) of the combined layers, consisting of 27 nm Al_2O_3 and 20 nm TaN. Different EUVL absorbers containing TaN, Ta, and Cr were compared,[254] with Ta-based material showing superiority to Cr-based one, and TaN being the best for optical characteristics, while Ta had the best performance on the geometric characterization in the studies.[254] Accurate evaluation is difficult because characteristics depend on the study conditions and process tools. Contrast measurements of reflection masks with Cr and Ta absorbers for EUVL show that reflectance on the reflecting and the absorbing part of the process patterns were 59% and 4.9%, respectively, on a Cr absorber mask, and 50% and 0.48%, respectively, on a Ta mask.[255] That means the contrasts were 12 for Cr mask and 105 for Ta mask. For Be-based multilayer (11.5 nm wavelength), the mask structure of TaSiN absorber, SiON repair buffer, and Cr conductive etch stop layer was reported.[256] Other absorber material candidates include Al–Cu, Ti, and TiN.[257,258] Till now, TaBN and TaN are the leading candidates for EUV mask absorbers.

The original buffer material was SiO_2, but it exhibited low etch selectivity to the silicon capping layer when etched using fluorine chemicals. Later, a ruthenium buffer was used

to improve this property.[259] Ruthenium also has a lower etch rate when an EUVL mask is repaired using focused ion beam.

EUVL mask fabrication will use the same technology as that for current 193 nm optical masks with some special requirements. One of them is the thickness of the absorber layer. The reflective EUV mask requires illumination of the mask at an oblique incident angle, which shifts the image on the wafer. Study shows that absorber thickness uniformity should be controlled within ±1 nm over the entire mask to minimize the CD impact of variations in reflectance swing.[260] This requirement is a challenge for mask fabrication steps, such as plasma etch, cleaning, and resist strip.

Temperature control during EUV mask fabrication is also required to avoid property changes and damage, e.g., process temperature should not exceed 150 °C. Pattern control, such as CD uniformity and CD mean to target (MTT) is extremely difficult. Much stricter specifications for EUVL masks at the 32 or 22 nm node than for the current optical photomask of the 65 nm node will mean that EUVL mask pattern control must rely on a new approach or technology.

Based on the present approach, EUV mask fabrication will continue using electron beam (e-beam) and CAR for pattern generation. This technology is already challenging at the current 65 nm and impending 45 nm technology nodes. CD uniformity and MTT are not expected to improve significantly using the same technology. Consequently, much stricter specifications for EUVL masks will burden the pattern transfer process, i.e., they will require EUV mask etch with no visible systematic CD error and also an almost zero etch CD bias, e.g., less than 3 nm. This necessitates a new method for etching the EUV mask.

Presently main etch CD error and bias result from soft mask, i.e., the limited etch selectivity between the working layer and the photoresist. Therefore, hard mask may be the only option for EUV mask pattern generation and transfer. Because direct pattern generation on hard mask (resistless) is not technologically mature, most applications using a hard mask have to generate the pattern on photoresist first, then transfer it to the hard mask, and finally transfer it to the working layer from the hard mask.

Various hard masks have been proposed.[261,262] Among them, the regular hard mask will make the process much more complicated, with manufacturing errors accumulating and possibly low yields. A major concern is the incomplete strip of this hard film after the absorber etch and resist strip.

Self-mask shows promising results. It uses a multistep etch on the absorber layer.[262,263] The first step etches through the antireflective (AR) sublayer using one set of etch conditions in terms of power and etch gaseous composition. The second etches the bulk absorber sublayer using another condition with adequate selectivity between the bulk absorber sublayer and the AR sublayer. In effect, the AR sublayer functions as the hard mask for the underlying bulk sublayer. Because the AR sublayer is very thin, the etch bias on it can be controlled to less than 3 nm, or almost "zero etch CD bias." Because of the high selectivity between bulk absorber and AR sublayers, CD does not change significantly, which ensures that the etch CD bias is determined mainly by the etch of the thin AR layer. Figure 9 shows a cross-sectional image of EUV mask fabricated using this method.[264]

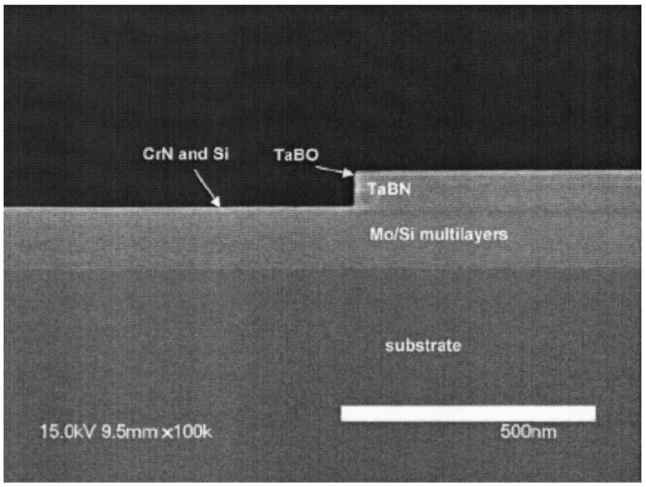

FIG. 9. Cross-sectional image of an EUV mask using TaBO/TaBN absorber.

For masks in current use, AR is always required for mask inspection and wafer printing. Hence the self-mask method adds no extra process or materials to the regular mask process. This makes the self-mask process very simple and easy to control. The key is to select etch chemicals correctly based on the composition of the AR and bulk absorber sublayers of the EUV mask. It was reported that thermodynamic calculation is very helpful in selecting the appropriate chemical system to obtain volatile products and ensure the self-mask function.[262,264]

VIII. CONCLUSION

Since it was first proposed in 1988, EUV lithography has been the subject of numerous intensive studies. Thus far, many technological challenges have been overcome, but many improvements are needed for practical application. Adoption time is mainly dependent on investment in research and development, driven by the extension of current optical lithography. In the 1990s, EUVL was targeted for the 100 nm node and below. However, 248 nm KrF lithography pushed optical lithography to the 90 nm node, and then 193 nm ArF lithography pushed it to 65 nm, with possible extension even to 45 and 32 nm, even though EUVL was widely accepted as the most promising NGL technology.

Lithography using 193 nm ArF and immersion is enabling optical lithography at the 45 nm technology node. Furthermore, 193 nm ArF with immersion technology as well as double patterning has been proposed for the 32 nm node. However, this technology is unlikely to be suitable beyond the 32 nm node due to extremely challenges such as alignment and overlay accuracy, and availability of high index materials and immersion liquid.

Prospects are good for EUVL to be in pilot production at the 32 nm node and in full-scale production at the 22 nm

node. With high NA and resolution enhancement technique (RET) on EUVL, it is very possible to push EUVL out by another technology node. Based on this prediction, a two-generation node lithography technology will be strongly competitive. The future of EUVL is strongly dependent on the extension of optical lithography.

Some current challenges in EUVL are common to all NGL technologies, such as resist resolution and LER. All NGLs must solve these problems. Some challenges are unique to EUVL, e.g., resist outgassing, owing to the EUVL high-vacuum environment.

Like other lithography technologies, EUVL consists of exposure tool technology, resist technology, and mask technology. So far, the collector and projection optics almost meet specifications, except for flare control. The key challenges are EUV source power, lifetime, and the degradation of the condenser. EUV source power also affects resist technology. Higher EUV source power will release the pressure to improve resist sensitivity. Recent progress on LPP EUV source shows a very promising result of 50 W EUV in-band power at intermediate focus, with expectation of 100 W at the end of 2007.

EUVL resist technology development is dependent on exposure tool development. After the small-field exposure tool became available, progress in developing EUVL resists was significant. By spring 2007, 25 nm 1:1 line:space line resolution and 20 nm 1:4 line:space were obtained on CAR, which removed the showstopper to implementing EUVL. Resist absorption of EUV and the effects on resist profile are also challenging. Sensitivity and LER also need improvement. The critical challenge is to meet requirement on resist resolution, sensitivity, and LER simultaneously.

EUVL masks may be the most challenging aspect of this new technology. Although EUVL masks require complicated multilayer, capping layer, buffer, and absorber, it is relatively "easy" to fabricate compared with other NGLs that use membrane masks. EUVL mask is a big challenge, but it is workable. EUVL mask technology includes mask blank preparation and pattern fabrication, as well as the use of nonpellicle masks. Defect-free EUVL mask is a critical challenge.

EUVL mask pattern generation and transfer face issues similar to those for other NGLs. Pattern transfer fidelity is also a challenge. For nonpellicle masks, movable pellicle and thermophoretic protection are being investigated; much more progress has to be made for this technology to become practical.

To summarize in one sentence, EUV lithography will not be "never seen," as joked about at the 2005 BACUS Symposium, but will be seen in the next few years.

[1]N. Kaiser, S. Yulin, T. Feigl, H. Bernitzki, and H. Lauth, Proc. SPIE **5250**, 109 (2004).
[2]A. M. Hawryluk and L. G. Seppala, J. Vac. Sci. Technol. B **6**, 2162 (1988).
[3]H. Kinoshita, K. Kuirhara, Y. Ishii, and Y. Torii, J. Vac. Sci. Technol. B **7**, 1648 (1989).
[4]J. E. Bjorkholm, J. Bokor, L. Eichner, and R. R. Freeman, J. Vac. Sci. Technol. B **8**, 1509 (1990).
[5]D. A. Tichenor, G. D. Kubiak, M. E. Malinowski, and R. H. Stulen, Opt. Lett. **16**, 1557 (1991).
[6]R. H. Stulen, IEEE J. Sel. Top. Quantum Electron. **1**, 970 (1995).
[7]A. M. Hawryluk and N. M. Ceglio, in *OSA Proceedings on Extreme Ultraviolet Lithography*, Monterey, CA, 19–21 September 1994, edited by Frits Zernike and David T. Atwood (Optical Society of America, Washington, DC, 1995), ISBN: 1-55752-363-0, Vol. 23, p. 13.
[8]D. R. Kania, D. P. Gaines, M. Hermann, and J. Honig, in *OSA Proceedings on Extreme Ultraviolet Lithography*, Monterey, CA, 19–21 September 1994, edited by Frits Zernike and David T. Atwood (Optical Society of America, Washington, DC, 1995), ISBN: 1-55752-363-0, Vol. 23, p. 234.
[9]M. Mermann, J. Honig, and L. Hackel, in *OSA Proceedings on Extreme Ultraviolet Lithography*, Monterey, CA, 19–21 September 1994, edited by Frits Zernike and David T. Atwood (Optical Society of America, Washington, DC, 1995), ISBN: 1-55752-363-0, Vol. 23, p. 238.
[10]R. C. Spitzer and D. P. Gaines, in *OSA Proceedings on Extreme Ultraviolet Lithography*, Monterey, CA, 19–21 September 1994, edited by Frits Zernike and David T. Atwood (Optical Society of America, Washington, DC, 1995), ISBN: 1-55752-363-0, Vol. 23, p. 243.
[11]G. D. Kubiak, K. D. Kren, K. W. Berger, T. G. Trucano, P. W. Fisher, and M. J. Gouge, in *OSA Proceedings on Extreme Ultraviolet Lithography*, Monterey, CA, 19–21 September 1994, edited by Frits Zernike and David T. Atwood (Optical Society of America, Washington, DC, 1995), ISBN: 1-55752-363-0, Vol. 23, p. 248.
[12]A. M. Hawryluk, D. R. Kania, P. Celliers, L. DaSilva, A. Stith, D. Stewart, and S. Mrowka, in *OSA Proceedings on Extreme Ultraviolet Lithography*, Monterey, CA, 19–21 September 1994, edited by Frits Zernike and David T. Atwood (Optical Society of America, Washington, DC, 1995), ISBN: 1-55752-363-0, Vol. 23, p. 204.
[13]D. R. Kania, F. J. Weber, S. P. Veron, A. Hawryluk, and S. L. Baker, in *OSA Proceedings on Extreme Ultraviolet Lithography*, Monterey, CA, 19–21 September 1994, edited by Frits Zernike and David T. Atwood (Optical Society of America, Washington, DC, 1995), ISBN: 1-55752-363-0, Vol. 23, p. 217.
[14]S. P. Vermon, M. J. Carey, D. P. Gaines, and F. J. Weber, in *OSA Proceedings on Extreme Ultraviolet Lithography*, Monterey, CA, 19–21 September 1994, edited by Frits Zernike and David T. Atwood (Optical Society of America, Washington, DC, 1995), ISBN: 1-55752-363-0, Vol. 23, p. 33.
[15]D. P. Gaines, S. P. Vermon, G. E. Sommargren, and D. R. Kania, in *OSA Proceedings on Extreme Ultraviolet Lithography*, Monterey, CA, 19–21 September 1994, edited by Frits Zernike and David T. Atwood (Optical Society of America, Washington, DC, 1995), ISBN: 1-55752-363-0, Vol. 23, p. 41.
[16]K. Skulina, C. Alford, R. Bionta, D. Makowiecki, E. M. Gullikson, R. Soufli, J. B. Kortright, and J. H. Underwood, in *OSA Proceedings on Extreme Ultraviolet Lithography*, Monterey, CA, 19–21 September 1994, edited by Frits Zernike and David T. Atwood (Optical Society of America, Washington, DC, 1995), ISBN: 1-55752-363-0, Vol. 23, p. 52.
[17]C. Cerjan, in *OSA Proceedings on Extreme Ultraviolet Lithography*, Monterey, CA, 19–21 September 1994, edited by Frits Zernike and David T. Atwood (Optical Society of America, Washington, DC, 1995), ISBN: 1-55752-363-0, Vol. 23, p. 142.
[18]D. P. Gaines, S. P. Vermon, G. E. Sommargren, and D. Fuchs, in *OSA Proceedings on Extreme Ultraviolet Lithography*, Monterey, CA, 19–21 September 1994, edited by Frits Zernike and David T. Atwood (Optical Society of America, Washington, DC, 1995), ISBN: 1-55752-363-0, Vol. 23, p. 171.
[19]G. E. Sommargren, in *OSA Proceedings on Extreme Ultraviolet Lithography*, Monterey, CA, 19–21 September 1994, edited by Frits Zernike and David T. Atwood (Optical Society of America, Washington, DC, 1995), ISBN: 1-55752-363-0, Vol. 23, p. 103.
[20]S. J. Cohen and L. G. Seppala, in *OSA Proceedings on Extreme Ultraviolet Lithography*, Monterey, CA, 19–21 September 1994, edited by Frits Zernike and David T. Atwood (Optical Society of America, Washington, DC, 1995), ISBN: 1-55752-363-0, Vol. 23, p. 109.
[21]S. P. Vermon and S. L. Baker, in *OSA Proceedings on Extreme Ultraviolet Lithography*, Monterey, CA, 19–21 September 1994, edited by Frits Zernike and David T. Atwood (Optical Society of America, Washington, DC, 1995), ISBN: 1-55752-363-0, Vol. 23, p. 222.
[22]P. D. Rockett, J. A. Hunter, G. D. Kubiak, K. Krenz, H. S. Shields, and M. Powers, in *OSA Proceedings on Extreme Ultraviolet Lithography*, Monterey, CA, 19–21 September 1994, edited by Frits Zernike and David

T. Atwood (Optical Society of America, Washington, DC, 1995), ISBN: 1-55752-363-0, Vol. 23, p. 255.
[23]K. B. Nguyen, P. Resnick, B. Draper, P. Mahl, J. H. Underwood, D. Chen, and P. Denham, in *OSA Proceedings on Extreme Ultraviolet Lithography*, Monterey, CA, 19–21 September 1994, edited by Frits Zernike and David T. Atwood (Optical Society of America, Washington, DC, 1995), ISBN: 1-55752-363-0, Vol. 23, p. 209.
[24]A. K. Ray-Chaudhuri, R. H. Stulen, W. Ng, and F. Certina, in *OSA Proceedings on Extreme Ultraviolet Lithography*, Monterey, CA, 19–21 September 1994, edited by Frits Zernike and David T. Atwood (Optical Society of America, Washington, DC, 1995), ISBN: 1-55752-363-0, Vol. 23, p. 161.
[25]D. A. Tichenor, A. K. Ray-Chaudhuri, G. D. Kubiak, and S. J. Haney, in *OSA Proceedings on Extreme Ultraviolet Lithography*, Monterey, CA, 19–21 September 1994, edited by Frits Zernike and David T. Atwood (Optical Society of America, Washington, DC, 1995), ISBN: 1-55752-363-0, Vol. 23, p. 89.
[26]W. C. Sweatt and W. W. Chow, in *OSA Proceedings on Extreme Ultraviolet Lithography*, Monterey, CA, 19–21 September 1994, edited by Frits Zernike and David T. Atwood (Optical Society of America, Washington, DC, 1995), ISBN: 1-55752-363-0, Vol. 23, p. 126.
[27]T. D. Nguyen, C. Khan-Malek, and J. H. Underwood, in *OSA Proceedings on Extreme Ultraviolet Lithography*, Monterey, CA, 19–21 September 1994, edited by Frits Zernike and David T. Atwood (Optical Society of America, Washington, DC, 1995), ISBN: 1-55752-363-0, Vol. 23, p. 56.
[28]J. H. Underwood, E. M. Gullikson, W. Ng, A. Ray-Chaudhuri, and F. Cerrina, in *OSA Proceedings on Extreme Ultraviolet Lithography*, Monterey, CA, 19–21 September 1994, edited by Frits Zernike and David T. Atwood (Optical Society of America, Washington, DC, 1995), ISBN: 1-55752-363-0, Vol. 23, p. 61.
[29]K. A. Goldberg, R. Beguiristain, J. Bokor, and H. Medecki, in *OSA Proceedings on Extreme Ultraviolet Lithography*, Monterey, CA, 19–21 September 1994, edited by Frits Zernike and David T. Atwood (Optical Society of America, Washington, DC, 1995), ISBN: 1-55752-363-0, Vol. 23, p. 134.
[30]D. C. Lee and A. R. Neureuther, in *OSA Proceedings on Extreme Ultraviolet Lithography*, Monterey, CA, 19–21 September 1994, edited by Frits Zernike and David T. Atwood (Optical Society of America, Washington, DC, 1995), ISBN: 1-55752-363-0, Vol. 23, p. 116.
[31]D. L. Windt and W. K. Waskiewicz, in *OSA Proceedings on Extreme Ultraviolet Lithography*, Monterey, CA, 19–21 September 1994, edited by Frits Zernike and David T. Atwood (Optical Society of America, Washington, DC, 1995), ISBN: 1-55752-363-0, Vol. 23, p. 47.
[32]Z. Tan, A. A. MacDowell, B. La Fontaine, and J. Russo, in *OSA Proceedings on Extreme Ultraviolet Lithography*, Monterey, CA, 19–21 September 1994, edited by Frits Zernike and David T. Atwood (Optical Society of America, Washington, DC, 1995), ISBN: 1-55752-363-0, Vol. 23, p. 151.
[33]B. La Fontaine, D. L. White, A. A. MacDowell, Z. Tan, D. M. Tennant, and O. R. Wood, in *OSA Proceedings on Extreme Ultraviolet Lithography*, Monterey, CA, 19–21 September 1994, edited by Frits Zernike and David T. Atwood (Optical Society of America, Washington, DC, 1995), ISBN: 1-55752-363-0, Vol. 23, p. 167.
[34]B. La Fontaine, A. A. McDowell, Z. Tan, G. N. Taylor, D. L. White, D. M. Tennant, and O. R. Wood II, in *OSA Proceedings on Extreme Ultraviolet Lithography*, Monterey, CA, 19–21 September 1994, edited by Frits Zernike and David T. Atwood (Optical Society of America, Washington, DC, 1995), ISBN: 1-55752-363-0, Vol. 23, p. 177.
[35]O. R. Wood, J. E. Bjorkholm, K. F. Dreyer, L. Fetter, and M. D. Himel, in *OSA Proceedings on Extreme Ultraviolet Lithography*, Monterey, CA, 19–21 September 1994, edited by Frits Zernike and David T. Atwood (Optical Society of America, Washington, DC, 1995), ISBN: 1-55752-363-0, Vol. 23, p. 83.
[36]Gary N. Taylor, R. S. Hutton, S. M. Stein, C. H. Boyce, B. La Fontaine, A. MacDowell, and D. R. Wheeler, in *OSA Proceedings on Extreme Ultraviolet Lithography*, Monterey, CA, 19–21 September 1994, edited by Frits Zernike and David T. Atwood (Optical Society of America, Washington, DC, 1995), ISBN: 1-55752-363-0, Vol. 23, p. 182.
[37]F. Jin and M. Richardson, in *OSA Proceedings on Extreme Ultraviolet Lithography*, Monterey, CA, 19–21 September 1994, edited by Frits Zernike and David T. Atwood (Optical Society of America, Washington, DC, 1995), ISBN: 1-55752-363-0, Vol. 23, p. 260.
[38]M. Richardson and F. Jin, in *OSA Proceedings on Extreme Ultraviolet Lithography*, Monterey, CA, 19–21 September 1994, edited by Frits Zernike and David T. Atwood (Optical Society of America, Washington, DC, 1995), ISBN: 1-55752-363-0, Vol. 23, p. 265.
[39]F. Cerrina, in *OSA Proceedings on Extreme Ultraviolet Lithography*, Monterey, CA, 19–21 September 1994, edited by Frits Zernike and David T. Atwood (Optical Society of America, Washington, DC, 1995), ISBN: 1-55752-363-0, Vol. 23, p. 280.
[40]B. M. Lum and A. R. Neureuther, in *OSA Proceedings on Extreme Ultraviolet Lithography*, Monterey, CA, 19–21 September 1994, edited by Frits Zernike and David T. Atwood (Optical Society of America, Washington, DC, 1995), ISBN: 1-55752-363-0, Vol. 23, p. 184.
[41]K. B. Nguyen, D. T. Attwood, T. Mizota, T. Haga, and H. Kinoshita, in *OSA Proceedings on Extreme Ultraviolet Lithography*, Monterey, CA, 19–21 September 1994, edited by Frits Zernike and David T. Atwood (Optical Society of America, Washington, DC, 1995), ISBN: 1-55752-363-0, Vol. 23, p. 193.
[42]Y. Saito, in *OSA Proceedings on Extreme Ultraviolet Lithography*, Monterey, CA, 19–21 September 1994, edited by Frits Zernike and David T. Atwood (Optical Society of America, Washington, DC, 1995), ISBN: 1-55752-363-0, Vol. 23, p. 227.
[43]H. Takenaka, T. Kawamura, Y. Ishii, T. Haga, and H. Kinoshita, in *OSA Proceedings on Extreme Ultraviolet Lithography*, Monterey, CA, 19–21 September 1994, edited by Frits Zernike and David T. Atwood (Optical Society of America, Washington, DC, 1995), ISBN: 1-55752-363-0, Vol. 23, p. 26.
[44]K. Murakami, H. Nagata, M. Ohtani, H. Oizumi, Y. Yamashita, and N. Atoda, in *OSA Proceedings on Extreme Ultraviolet Lithography*, Monterey, CA, 19–21 September 1994, edited by Frits Zernike and David T. Atwood (Optical Society of America, Washington, DC, 1995), ISBN: 1-55752-363-0, Vol. 23, p. 122.
[45]P. Kuerz, T. Boehm, H. J. Mann, and S. Muellender, Presentation on SEMATECH Fifth EUVL Symposium, 2006, on internet (http://www.sematech.org/meetings/archives/litho/euvl/7870/index.htm).
[46]P. J. Silverman, J. Microlithogr., Microfabr., Microsyst. **4**, 011006 (2005).
[47]P. Silverman, Proc. SPIE **4343**, 12 (2001).
[48]D. Tichenor, A. K. Ray-Chaudhuri, W. C. Replogle, and R. H. Stulen, Proc. SPIE **4343**, 19 (2001).
[49]D. A. Tichenor, A. K. Ray-Chaudhuri, S. H. Lee, and H. N. Chapman, Proc. SPIE **4506**, 9 (2001).
[50]H. N. Chapman, A. K. Ray-Chaudhuri, D. A. Tichenor, and W. C. Replogle, J. Vac. Sci. Technol. B **19**, 2389 (2001).
[51]D. A. Tichenor, G. D. Kubiak, W. C. Replogle, and L. E. Klebanoff, Proc. SPIE **3997**, 48 (2000).
[52]W. P. Bllard, K. A. Tichenor, D. J. O'Connell, and L. J. Bernardez II, Proc. SPIE **5037**, 47 (2003).
[53]S. H. Lee, D. A. Tichenor, W. P. Ballard, and L. J. Bernardez II, Proc. SPIE **4688**, 266 (2002).
[54]J. P. H. Benschop, U. Dinger, and D. C. Ockwell, Proc. SPIE **3997**, 34 (2000).
[55]H. Meiling, J. Benschop, U. Dinger, and P. Kurz, Proc. SPIE **4343**, 38 (2001).
[56]H. Meining, H. Meijer, V. Banine, and R. Moors, Proc. SPIE **6151**, 615108 (2006).
[57]K. Ota, K. Murakami, H. Kondo, T. Oshino, K. Sugisaki, and H. Komatsuda, Proc. SPIE **4343**, 60 (2001).
[58]T. Miura, K. Murakami, K. Suzuki, Y. Kohama, K. Morita, K. Hada, and T. Ohkubo, Proc. SPIE **6517**, 651707 (2007).
[59]T. Miura, K. Murakami, K. Suzuki, Y. Kohama, Y. Ohkubo, and T. Asami, Proc. SPIE **6151**, 615105 (2006).
[60]J. M. Roberts, T. Bacuita, R. L. Bristol, and H. B. Cao, Proc. SPIE **5751**, 64 (2005).
[61]P. Naulleau, K. A. Goldberg, E. Anderson, and J. P. Cain, Proc. SPIE **5751**, 56 (2005).
[62]A. Brunton, J. Cashmore, P. Elbourn, and G. Elliner, Proc. SPIE **5374**, 869 (2004).
[63]M. Booth, O. Brioso, A. Brunton, and J. Cashmore, Proc. SPIE **5751**, 78 (2005).
[64]H. Oizumi, Y. Tanaka, F. Kumasaka, and I. Nishiyama, Proc. SPIE **5751**, 102 (2005).
[65]S. Uzawa, H. Kubo, Y. Miwa, T. Tsuji, and H. Morishima, Proc. SPIE **6517**, 651708 (2007).
[66]V. Banine and R. Moors, J. Phys. D **37**, 3207 (2004).
[67]T. Krucken, K. Bergmann, L. Juschkin, and R. Lebert, J. Phys. D **37**,

3213 (2004).
[68]K. Fahy, P. Kunne, L. McKinney, and G. O'Sullivan, J. Phys. D **37**, 3225 (2004).
[69]B. A. M. Hansson and H. Hertz, J. Phys. D **37**, 3233 (2004).
[70]U. Stamm, J. Phys. D **37**, 3244 (2004).
[71]V. M. Borisov, A. V. Eltsov, A. S. Ivanov, and Y. B. Kiryukhin, J. Phys. D **37**, 3254 (2004).
[72]I. V. Fomenko, N. Bowering, C. L. Rettig, and S. T. Melnychuk, J. Phys. D **37**, 3266 (2004).
[73]M. W. McGeoch, J. Phys. D **37**, 3277 (2004).
[74]W. T. Silfvast, IEEE J. Sel. Top. Quantum Electron. **35**, 700 (1999).
[75]B. A. M. Hansson, I. V. Fomenkov, and N. R. Bowering, Proc. SPIE **6151**, 61510R (2006).
[76]Y. Teramoto, G. Niimi, and D. Yamatani, Proc. SPIE **6151**, 615147 (2006).
[77]L. A. Shmaenok, F. Bijkerk, C. Bruineman, R. K. F. Bastiaensen, A. P. Shevelko, D. M. Simanovskii, A. N. Gladskikh, and S. V. Bobashev, Proc. SPIE **2523**, 113 (1995).
[78]G. D. Kubiak, D. A. Tichenor, and R. H. Stulen, Technical Digest, CLEO/Pacific Rim'95, *The Pacific Rim Conference on Lasers and Electro-Optics*, Chiba, Japan, 11–14 July, 1995 (Optical Society of America, Washington, DC, 1995), Vol. 1, p. 45.
[79]B. A. M. Hansson, L. Rymell, M. Berglund, O. Hembert, E. Janin, J. Thoresen, and H. M. Hertz, Proc. SPIE **4506**, 1 (2001).
[80]G. F. Kooijman, R. de Bruijn, K. Koshelev, F. Bijkerk, W. Shailh, A. J. Bodey, and G. Hirst, Lasers For Science Facility Programme-Physics **2002**, 142 (2002).
[81]A. Endo, H. Hoshino, T. Ariga, and T. Miura, Proc. SPIE **5918**, 591801 (2005).
[82]U. Vogt, H. Stiel, I. Will, and M. Wieland, Proc. SPIE **4343**, 535 (2001).
[83]Y. Teramoto, Z. Narihiro, D. Yamatami, and T. Yokoyama, Proc. SPIE **6517**, 65173R (2007).
[84]B. E. Jurczyk, D. S. Alman, E. L. Antonsen, and M. A. Jaworski, Proc. SPIE **5751**, 572 (2005).
[85]S. M. Owens, Proc. SPIE **5918**, 591807 (2005).
[86]V. M. Borisov, E. Ahmad, S. Goetze, and A. S. Ivanov, Proc. SPIE **4688**, 626 (2002).
[87]I. V. Fomenkov, W. N. Partlo, R. M. Ness, and I. R. Oliver, Proc. SPIE **4688**, 634 (2002).
[88]E. Robert, T. Gonthiez, O. Sarroukh, and A. L. Thomann, Proc. SPIE **4688**, 672 (2002).
[89]J. Pankert, K. Bergmann, J. Klein, and W. Neff, Proc. SPIE **5037**, 112 (2003).
[90]U. Stamm, I. Hama, I. Balogh, and H. Birner, Proc. SPIE **5037**, 119 (2003).
[91]M. W. McGeoch and C. T. Pike, Proc. SPIE **5037**, 141 (2003).
[92]R. Lebert, K. Bergmann, L. Juschkin, O. Rosier, and W. Neff, Proc. SPIE **4343**, 215 (2001).
[93]A. Hassanein, V. Sizyuk, V. Tolkach, V. Morozo, and B. Rice, J. Microlithogr., Microfabr., Microsyst. **3**, 130 (2004).
[94]A. Hassanein, T. Burtseva, J. N. Brooks, I. Konkashbaev, and B. Rice, Proc. SPIE **5037**, 358 (2003).
[95]U. Stamm, J. Kleinschmidt, K. Gabel, and G. Hergehan, Proc. SPIE **5751**, 236 (2005).
[96]U. Stamm, J. Kleinschmidt, and D. Bolshukhin, Proc. SPIE **6151**, 61510O (2006).
[97]U. Stamm, M. Yoshioka, J. Kleinschmidt, and C. Ziener, Proc. SPIE **6517**, 65170P (2007).
[98]D. C. Brandt, I. V. Fomenkov, A. I. Ershov, and W. N. Partlo, Proc. SPIE **6517**, 65170Q (2007).
[99]S. Bajt, J. Alamceda, T. Barbee, Jr., W. M. Clift, J. A. Folta, B. Kaufmann, and E. Spiller, Proc. SPIE **4506**, 65 (2001).
[100]U. Kleineberg, T. Westerwalbesloh, O. Wehmeyer, M. Sundermann, A. Brechling, U. Heinzmann, M. Haidl, and S. Mullender, Proc. SPIE **4506**, 113 (2001).
[101]B. W. Smith, P. Venkataraman, S. K. Kurinec, and R. S. Mackay, Proc. SPIE **3331**, 544 (1998).
[102]V. Banine, J. Benschop, M. Leeders, and R. Moors, Proc. SPIE **3997**, 126 (2000).
[103]N. Benoit, S. Yulin, T. Feigl, and N. Kaiser, Proc. SPIE **6317**, 63170K (2006).
[104]M. Ohring, *The Materials Science of Thin Films* (Academic Press, New York, 1992), pp. 416–420.
[105]G. G. Stoney, Proc. R. Soc. London, Ser. A **82**, 172 (1909).
[106]E. Louis, A. E. Yakshin, E. Zoethout, R. W. E. van de Kruijs, I. Nedelu, S. Alonso van der Westen, T. Tasarfati, and F. Bijkerk, Proc. SPIE **5900**, 590002 (2005).
[107]K. Murakami and M. Shiraisi, Proc. SPIE **4506**, 56 (2001).
[108]M. Shiraishi, W. Ishiyama, T. Oshino, and K. Murakami, Proc. SPIE **3997**, 620 (2000).
[109]M. Shiraishi, W. Ishiyama, N. Kandaka, T. Oshino, and K. Murakami, Proc. SPIE **4688**, 516 (2002).
[110]M. Shiraishi, N. Kandaka, and K. Murakami, Proc. SPIE **5037**, 249 (2003).
[111]T. Feigl, S. Yulin, N. Kaiser, and R. Thielsch, Proc. SPIE **3997**, 420 (2000).
[112]P. Nicolosi, A. Patelli, M. G. Pelizzo, V. Rigato, G. Maggioni, L. Depero, E. Bontempi, G. Mattei, L. Poletto, P. Mazzoldi, and G. Tondello, Proc. SPIE **4506**, 76 (2001).
[113]S. Bajt and D. G. Stearns, Appl. Opt. **44**, 7735 (2005).
[114]S. Bajt, H. N. Chapman, N. Nguyen, and J. Alameda,Proc. SPIE **5037**, 236 (2003).
[115]H. Over, Y. B. He, A. Farkas, G. Mellau, C. Korte, M. Knapp, M. Chandhok, and M. Fang, J. Vac. Sci. Technol. B **25**, 1123 (2007).
[116]P. B. Mirkarimi, Eberhard Spiller, Sherry L. Baker, Victor Sperry, Daniel G. Stearns, and Eric M. Gullikson, J. Microlithogr., Microfabr., Microsyst. **3**, 139 (2004).
[117]E. M. Gullikson, C. Cejan, D. G. Stearns, P. B. Mirkarimi, and D. W. Sweeney, J. Vac. Sci. Technol. B **20**, 81 (2001).
[118]T. Pistor, Y. Deng, and A. Neureuther, J. Vac. Sci. Technol. B **18**, 2926 (2000).
[119]E. Spiller, F. J. Weber, C. Montcalm, S. L. Baker, E. M. Gulikson, and J. H. Underwood, Proc. SPIE **3331**, 62 (1998).
[120]E. Zoethout, P. Suter, R. W. E. van de Kruiis, A. E. Yakshin, E. Louis, and F. Bijkerk, H. Enkisch, and S. Mullender, Proc. SPIE **5374**, 892 (2004).
[121]E. Louis, E. Zoethout, R. W. E. van de Kruijs, and I. Nedulcu, Proc. SPIE **5751**, 1170 (2005).
[122]K. Hiruma, S. Miyagaki, and H. Yamanashi, Proc. SPIE **6151**, 61511V (2006).
[123]E. Louis, M. J. H. den Hartog, E. L. G. Maas, and F. Bijkerk, Proc. SPIE **3331**, 400 (1998).
[124]H. Chapman and K. A. Nugent, Proc. SPIE **3767**, 225 (1999).
[125]P. Marczuk and W. Egle, Proc. SPIE **5533**, 145 (2004).
[126]R. J. Anderson, D. A. Buchenauer, K. A. Williams, and W. M. Clift, Proc. SPIE **5751**, 128 (2005).
[127]H. Meiling, V. Banine, P. Kurz, and N. Harned, Proc. SPIE **5374**, 31 (2004).
[128]J. P. Allain, M. Nieto, and A. Hassanein, Proc. SPIE **6151**, 615131 (2006).
[129]M. P. Kanouff and A. K. Ray-Chaudhuri, Proc. SPIE **3676**, 735 (1999).
[130]T. Feigl, S. Yulin, and N. Benoit, Proc. SPIE **6151**, 61514A (2006).
[131]N. R. Bowering, A. I. Ershov, and W. F. Marx, Proc. SPIE **6151**, 61513R (2006).
[132]N. Harned, M. Goethals, R. Groeneveld, and P. Kuerz, Proc. SPIE **6517**, 651706 (2007).
[133]E. M. Gullikson, S. Baker, J. E. Bjorkholm, and J. Boker, Proc. SPIE **3676**, 717 (1999).
[134]C. Krautschik, M. Chandhok, G. Zhang, S. Lee, and M. Goldstein, Proc. SPIE **5037**, 58 (2003).
[135]S. H. Lee, P. Naulleau, C. Krautschik, and M. Chandhok, Proc. SPIE **5037**, 103 (2003).
[136]M. Chandhok, S. H. Lee, C. Krautschik, B. J. Rice, E. Panning, M. Goldstein, and M. Shell, Proc. SPIE **5374**, 86 (2004).
[137]S. Hun Lee, Y. Shroff, and M. Chandhok, Proc. SPIE **5751**, 707 (2005).
[138]D. J. O'Connell, S. H. Lee, W. P. Ballard, and D. A. Techenor, Proc. SPIE **5037**, 83 (2003).
[139]S. Hun Lee, M. Chandhok, J. Roberts, and B. J. Rice, Proc. SPIE **5751**, 293 (2005).
[140]F. M. Schellenberg, J. Word, and O. Toublan, Proc. SPIE **5751**, 320 (2005).
[141]J. P. Cain, P. Naulleau, and C. J. Spanos, Proc. SPIE **5751**, 741 (2005).
[142]B. Mertens, B. Wolschrijn, R. Jansen, and N. Koster, Proc. SPIE **5037**, 95 (2003).
[143]R. Krurt, M. van Beek, C. Crombeen, P. Zalm, and Y. Tamminga, Proc. SPIE **4688**, 702 (2002).
[144]S. Graham, M. E. Malinowski, C. E. Steinhaus, P. A. Grunow, and L. E.

Klebanoff, Proc. SPIE **4688**, 431 (2002).
[145]M. Malinowski, P. Grunow, C. Steinhaus, M. Clift, and L. Klebanoff, Proc. SPIE **4343**, 347 (2001).
[146]E. Tejnil, K. A. Goldberg, S. Lee, H. Medecki, P. J. Batson, P. E. Denham, A. A. MacDowell, J. Bokor, and D. Attwood, J. Vac. Sci. Technol. B **15**, 2455 (1997).
[147]D. T. Attwood, G. Sommargren, R. Beguiristain, K. Nguyen, and J. Bokor, Appl. Opt. **32**, 7022 (1993).
[148]G. Seitz, S. Schulte, U. Dinger, O. Hocky, B. Fellner, and M. Rupp, Proc. SPIE **5533**, 20 (2004).
[149]M. Hasegawa, C. Ouchi, T. Hasegawa, and S. Kato, Proc. SPIE **5533**, 27 (2004).
[150]G. E. Sommargren, D. W. Phillion, M. A. Johnson, and N. Q. Nguyen, Proc. SPIE **4688**, 316 (2002).
[151]K. A. Goldberg, P. Naulleau, P. Denham, and S. B. Rekawa, Proc. SPIE **5037**, 69 (2003).
[152]C. Tarrio, T. B. Lucatorto, S. Grantham, M. B. Squires, U. Arp, and L. Deng, Proc. SPIE **4506**, 32 (2001).
[153]F. Scholze, J. Tummler, E. Gullikson, and A. Aquila, J. Microlithogr., Microfabr., Microsyst. **2**, 233 (2003).
[154]Y. Kakutani, M. Niibe, K. Kakiuchi, and H. Takase, Proc. SPIE **5533**, 47 (2004).
[155]K. Starke, H. Blaschke, L. Jensen, S. Nevas, and D. Ristau, Proc. SPIE **6317**, 631701 (2006).
[156]K. A. Lavery, K. W. Choi, and B. D. Vogt, Proc. SPIE **6153**, 615313 (2006).
[157]R. L. Jones, V. M. Prabhu, D. L. Goldfarb, E. K. Lin, C. L. Soles, J. L. Lenhart, W. L. Wu, and M. Angelopoulos, *Polymers for Microelectronics and Nanoelectronics*, edited by Q. Lin (American Chemical Society, Washington, DC, 2004), Vol. 874, pp. 86–97.
[158]J. Nakamura, H. Ban, and A. Tanaka, Jpn. J. Appl. Phys., Part 1 **31**, 4294 (1992).
[159]A. Jouve, J. Simon, A. Pikon, H. Solak, C. Vannuffel, and J.-H. Tortai, Proc. SPIE **6153**, 61531C (2006).
[160]K. Tanaka, R. Naito, T. Kitada, and Y. Kiba, Proc. SPIE **5039**, 1366 (2003).
[161]K. Yoshimoto, P. Stoykovich, H. B. Cao, J. J. de Pablo, P. F. Nealey, and W. J. Drugan, J. Appl. Phys. **96**, 1857 (2004).
[162]F. Tardif, *Cleaning Technology in Semiconductor Device Manufacturing VIII*, edited by J. Ruzyllo (Electrochemical Society, 2003), ISBN: 156677411X, p. 26.
[163]M. H. Jung, H. W. Kim, J. Hong, S. G. Woo, H. K. Cho, and W. S. Han, Proc. SPIE **5376**, 1100 (2004).
[164]D. L. Goldfarb, J. J. de Pablo, P. F. Nealey, J. P. Simons, W. M. Moreau, and M. Angelopoulos, J. Vac. Sci. Technol. B **18**, 3313 (2000).
[165]H. Namatsu, Proc. SPIE **4688**, 888 (2002).
[166]ITRS, International Technology Roadmap for Semiconductors 2004 Update (2004).
[167]H. B. Cao and P. F. Nealey, J. Vac. Sci. Technol. B **18**, 3303 (2000).
[168]P. Zhang, M. Jaramillo, Jr., D. J. King, M. B. Rao, B. L. O'Brien, and B. F. Ross, Proc. SPIE **5376**, 807 (2004).
[169]I. Junarsa, M. P. Stoykovich, K. Yoshimoto, and P. F. Nealey, Proc. SPIE **5376**, 842 (2004).
[170]R. Peters, C. Parker, J. Cobb, E. Luckowski, E. Weisbrod, and B. Dauksher, Proc. SPIE **5376**, 746 (2005).
[171]M. Wagner, J. DeYoung, and D. Harbinson, Proc. SPIE **6153**, 61531I (2006).
[172]V. Constantoudis, E. Gogolides, and G. P. Patsis, Proc. SPIE **6153**, 61533W (2006).
[173]J. DeYoung, M. Wagner, C. Harbinson, M. Miles, A. Zweber, and R. Carbonell, Proc. SPIE **6153**, 615345 (2006).
[174]W. Yueh, H. B. Cao, V. Thiumala, and H. Choi, Proc. SPIE **5753**, 765 (2005).
[175]S. Masuda, S. Kamimura, S. Hirano, W. Hoshino, and K. Mizutani, Proc. SPIE **6519**, 65191O (2007).
[176]H. Cao, W. Yueh, B. Rice, J. Roberts, T. Bacuita, and M. Chandhok, Proc. SPIE **5376**, 757 (2005).
[177]J. M. Hutchinson, Proc. SPIE **3331**, 531 (1998).
[178]V. Rao, J. Cobb, C. Henderson, and O. Okoroanynwu, Proc. SPIE **3676**, 615 (1999).
[179]R. Brainard, P. Trefonas, J. H. Lammers, and C. A. Cutler, Proc. SPIE **5374**, 74 (2004).
[180]J. Pablo Bravo-Vasquez, Y. J. Kwark, C. K. Ober, H. B. Cao, and H. Deng, Proc. SPIE **5753**, 732 (2005).
[181]J. Dai and C. K. Ober, Proc. SPIE **5376**, 508 (2005).
[182]J. Pablo Bravo-Vasquez, Y. J. Kwark, C. K. Ober, H. B. Cao, H. Deng, and R. Meagley, Proc. SPIE **5376**, 739 (2005).
[183]C. Henderson, D. Wheeler, T. Pollagi, and D. O'Connell, Proc. SPIE **3331**, 32 (1998).
[184]N. Matsuzawa and H. Oizumi, Presentation on SEMATECH First EUVL Workshop, 1999 on internet (http://ismi.sematech.org/meetings/archives/litho/euvl/199910XX/index.htm).
[185]A. De Silva, Dreq Forman, and Christopher K. Ober, Proc. SPIE **6153**, 615341 (2006).
[186]J. Dai, C. K. Ober, L. Wang, F. Oerrina, and P. Nealey, Proc. SPIE **4690**, 1193 (2002).
[187]J. Dai, C. K. Ober, S. O. Kim, and P. Nealey, Proc. SPIE **5039**, 1164 (2003).
[188]P. Dentinger, G. Cardinale, C. Henderson, A. Fisher, and A. Ray-Chaudhuri, Proc. SPIE **3997**, 588 (2000).
[189]L. B. Cao, W. Yueh, J. Boberts, B. Rice, R. Bristol, and M. Chandhok, Proc. SPIE **5753**, 459 (2005).
[190]H. Oizumi, Y. Tanaka, F. Kumasaka, and I. Nishiyama, Proc. SPIE **6151**, 61512Q (2006).
[191]M. Wang, C. T. Lee, D. L. Henderson, W. Yueh, J. M. Roberts, and K. E. Gonsalves, Proc. SPIE **6519**, 65191F (2007).
[192]D. Shiono, H. Hada, H. Yukawa, and H. Oizumi, Proc. SPIE **6519**, 65193U (2007).
[193]J. W. Thackeray, R. A. Nassar, R. Brainard, and D. Goldfarb, Proc. SPIE **6517**, 651719 (2007).
[194]Y. Tanaka, H. Oizumi, and Y. Kikuchi, Proc. SPIE **6151**, 61512S (2006).
[195]A. R. Stivers, P. Y. Yan, G. Zhang, E. Liang, E. Y. Shu, E. Tejnil, B. Lieberman, R. Nagpal, K. Hsia, M. Penn, and F. C. Lo, Proc. SPIE **5567**, 13 (2004).
[196]C. Constancias, M. Richard, and D. Joyeux, Proc. SPIE **6151**, 61511W (2006).
[197]S. I. Han, J. R. Wasson, P. J. S. Mangat, J. L. Cobb, K. Lucas, and S. D. Hector, Proc. SPIE **4688**, 481 (2002).
[198]S. I. Han, E. Weisbrod, Q. Xie, P. J. S. Mangat, S. D. Hector, and W. J. Dauksher, Proc. SPIE **5037**, 314 (2003).
[199]B. La Fontaine, A. R. Pawloski, O. Wood, and Y. Deng, Proc. SPIE **6156**, 61510A (2006).
[200]B. La Fontaine, Presentation on SEMATECH Fifth EUVL Symposium, 2006 on internet (http://www.sematech.org/meetings/archives/litho/euvl/7870/index.htm).
[201]A. Chiba, M. Sugawara, and I. Nishiyama, Proc. SPIE **5037**, 841 (2003).
[202]M. Kawata, A. Takada, H. Hayashi, N. Sugimoto, and S. Kikugawa, Proc. SPIE **6151**, 61511A (2006).
[203]W. Rosch, L. Beall, J. Maxon, R. Sabia, and R. Sell, Proc. SPIE **6151**, 615122 (2006).
[204]P. Seidel, Proc. SPIE **6607**, 66070I (2007).
[205]M. Nataraju, J. Sohn, A. R. Mikkelson, K. T. Turner, R. L. Engelstad, and C. K. Van Peski, Proc. SPIE **6151**, 61510C (2006).
[206]M. C. Lam and A. R. Neureuther, Proc. SPIE **6151**, 61510D (2006).
[207]M. Bujak *et al.*, Proc. SPIE **3665**, 30 (1999).
[208]S. Burkhart, C. Cerjan, P. Kearney, P. Mirkarimi, C. Walton, and A. Ray-Chaudhuri, Proc. SPIE **3676**, 570 (1999).
[209]J. A. Folta, J. C. Davidson, C. C. Larson, C. C. Walton, and P. A. Kearney, Proc. SPIE **4688**, 173 (2002).
[210]Y. Tezuka, M. Ito, T. Terasawa, and T. Tomie, Proc. SPIE **5374**, 271 (2004).
[211]A. Ma, P. Kearney, D. Krick, and R. Randive, Proc. SPIE **5751**, 168 (2005).
[212]P. Seidel, Proc. SPIE **5751**, 178 (2005).
[213]T. Liang, Edita Tejnil, and Alan Stivers, Proc. SPIE **4889**, 1065 (2002).
[214]T. Liang, A. Stivers, P. Y. Yan, E. Tejnil, and G. Zhang, Proc. SPIE **4562**, 288 (2002).
[215]E. Tejnil, E. Gullikson, and A. R. Stivers, Proc. SPIE **5567**, 943 (2004).
[216]S. Jeong *et al.*, J. Vac. Sci. Technol. B **16**, 3430 (1998).
[217]S. Jeong, L. Johnson, S. Rekawa, C. C. Walton, S. T. Prisbrey, E. Tejnil, J. H. Underwood, and J. Bokor, J. Vac. Sci. Technol. B **17**, 3009 (1999).
[218]E. Tejnil and Alan Stivers, Proc. SPIE **3873**, 792 (1999).
[219]T. Haga, H. Takenaka, and M. Fukuda, J. Vac. Sci. Technol. B **18**, 2916 (2000).
[220]S. S. Kim, J. Par, and R. Chalykh, Proc. SPIE **6151**, 61511C (2006).
[221]A. Stivers, T. Liang, M. Penn, and B. Lieberrman, Proc. SPIE **3889**, 408

(2002).
[222]J. P. Urbach, J. Cavelaars, H. Kusunose, T. Liang, and A. R. Stivers, Proc. SPIE **5256**, 556 (2003).
[223]L. E. Klebanoff and D. J. Rader, U.S. Patent No. 6153044 (28 November 2000).
[224]T. Tomie, T. Erasawa, Y. Tezuka, and M. Ito, Proc. SPIE **5038**, 41 (2003).
[225]Y. Tezuka, M. Ito, T. Terasawa, and T. Tomie, Proc. SPIE **5038**, 866 (2003).
[226]U. Kleineberg, J. Lin, and U. Neuhaeusler, Proc. SPIE **6151**, 615120 (2006).
[227]Y. Tezuka, M. Ito, T. Terasawa, and T. Tomie, Proc. SPIE **5567**, 791 (2004).
[228]S. S. Kim, R. Chalyck, S. G. Woo, and H. K. Cho, Proc. SPIE **5751**, 678 (2005).
[229]L. E. Klebanoff and D. J. Rader, U.S. Patent No. 6253464 (3 July 2001).
[230]D. J. Rader, D. E. Dedrick, E. W. Beyer, A. H. Leung, and L. E. Klenbanoff, Proc. SPIE **4688**, 182 (2002).
[231]D. E. Dedrick, E. W. Beyer, D. J. Rader, L. E. Klebanoff, and A. H. Leung, J. Vac. Sci. Technol. B **23**, 307 (2005).
[232]S. Hector and Pawitter Mangat, J. Vac. Sci. Technol. B **19**, 2612 (2001).
[233]Y. A. Shroff, M. Goldstein, B. Rice, S. H. Lee, K. V. Ravi, and D. Tanzil, Proc. SPIE **6151**, 615104 (2006).
[234]J. Rau, Hermann Wendt, Josef Mathuni, Christoph Stepper, Albrecht Ehrmann, and Frank-Michael Kamm, Proc. EMC **36**, 23 (2002).
[235]D. Bratton, Ramakrishnan Ayothi, Nelson Felix, Heidi Cao, Hai Deng, and Christopher K. Ober, Proc. SPIE **6153**, 61531D (2006).
[236]H. Nii, H. Kinoshita, T. Watanabe, K. Hamanoto, H. Tsubakino, and Y. Sugie, Proc. SPIE **4409**, 681 (2001).
[237]P. Mangat, S. Hector, S. Rose, G. Cardinale, E. Tejnil, and A. Stivers, Proc. SPIE **3997**, 76 (2000).
[238]G. Zhang and Pei-Yang Yan, Proc. SPIE **4889**, 1092 (2002).
[239]M. Oda, Akira Ozawa, and Hideo Yoshihara, J. Vac. Sci. Technol. B **11**, 37 (1993).
[240]W. J. Dauksher *et al.*, J. Vac. Sci. Technol. B **13**, 3104 (1995).
[241]K. Fujii, Yuusuke Tanaka, Toshiyuki Iwamoto, Shinji Tsuboi, Hiroaki Sumitani, Takao Taguchi, Katsumi Suzuki, andYasuji Matsui, Proc. SPIE **4343**, 155 (2001).
[242]Y. Tanaka, Kiyoshi Fujii, Kenichiro Suzuki, Toshiyuki Iwamoto, Shinji Tsuboi, and Yasuji Matsui, Proc. SPIE **4409**, 660 (2001).
[243]M. J. Lercel, Cameron J. Brooks, Douglas E. Benoit, and Maheswaran Surendra, J. Vac. Sci. Technol. B **16**, 3577 (1998).
[244]Y. Du, Chang Ju Choi, Guojing Zhang, She-Jin Park, Pei-Yang Yan, and Ki-Ho Baik, Proc. SPIE **6282**, 62833D (2006).
[245]H. Seitz *et al.*, Proc. SPIE **6151**, 615109 (2006).
[246]K. M. Lee, Malahat Tavassoli, Alan Stivers, and Barry Lieberman, Proc. SPIE **5992**, 59922B (2005).
[247]F. Letzkus, Joerg Butschke, Mathias Irmscher, Holger Sailer, Uwe Dersch, and Christian Holfeld, Proc. SPIE **5992**, 59922A (2005).
[248]M. Hosoya, Tsutomu Shoki, Takeru Kinoshita, Noriyuki Sakaya, and Osamu Nagarekawa, Proc. SPIE **5130**, 1026 (2003).
[249]P. Y. Yan, Guojing Zhang, Rajesh Nagpal, Emily Y. Shu, Chaoyang Li, Ping Qu, and Frederick Chen, Proc. SPIE **5567**, 774 (2004).
[250]T. Abe *et al.*, Proc. SPIE **6439**, 6439 (2006).
[251]T. Abe, Akiko Fujii, Hiroshi Mohri, and Naoya Hayashi, Proc. SPIE **6282**, 62830H (2006).
[252]S. Tamura, Koichiro Kanayama, Yasushi Nishiyama, Tadashi Matsuo, and Akira Tamura, Proc. SPIE **6282**, 62830J (2006).
[253]S. Yoon Lee, Tae Geun Kim, Chung Yong Kim, In-Yong Kang, Yong-Chae Chung, and Jinho Ahn, Proc. SPIE **6151**, 61511Y (2006).
[254]I. Y. Kang, J. Ahn, H. K. Oh, and Y. C. Chung, Proc. SPIE **6151**, 615121 (2006).
[255]M. Niibe, T. Watanabe, H. Nii, T. Tanaka, and H. Kinoshita, Jpn. J. Appl. Phys., Part 1 **39**, 6815 (2000).
[256]P. Mangat, James Wasson, Scott Hector, Greg Cardinale, and Sasa Bajt, Proc. SPIE **3997**, 814 (2000).
[257]P. Y. Yan, Guojing Zhang, Andy Ma, and Ted Liang, Proc. SPIE **4343**, 409 (2001).
[258]P. Y. Yan, Guojing Zhang, Patrick Kofron, Jeff Powers, Mark Tran, Ted Liang, Alan Stivers, and Fu-Chang Lo, Proc. SPIE **4066**, 116 (2000).
[259]B. T. Lee, E. Hoshino, M. Takahashi, and T. Yneda, Proc. SPIE **4343**, 746 (2001).
[260]F. T. Chen, Proc. SPIE **5037**, 347 (2003).
[261]D. Y. Chan, U.S. Patent No. 6472107 (29 October 2002).
[262]B. Wu, Proc. SPIE **5567**, 1195 (2004).
[263]B. Wu, J. Vac. Sci. Technol. B **24**, 1 (2006).
[264]B. Wu, A. Kumar, Appl. Phys. Lett. **90**, 063105 (2007).